Canadian Mineralogist
Vol. 26, pp. 675-696 (1988)

SULFIDE FORMATION AND HYDROTHERMAL ALTERATION OF HEMIPELAGIC SEDIMENT IN MIDDLE VALLEY, NORTHERN JUAN DE FUCA RIDGE

WAYNE D. GOODFELLOW
Geological Survey of Canada, 601 Booth Street, Ottawa, Ontario K1A 0E8
BERTRAND BLAISE
Pacific Geoscience Centre, Geological Survey of Canada, P.O. Box 6000, Sidney, British Columbia V8L 4B2

ABSTRACT

Middle Valley is a sedimented fault-bounded rift valley at the northern end of the Juan de Fuca Ridge. Sediment thicknesses are highly variable and increase from the margins to 1500 m in the center. Within the Valley, eight mound-like features up to 60 m high and several hundred meters across were observed with SeaMARC II acoustic imagery and Seabeam bathymetry. Two areas displaying anomalously high heat-flow values were actively venting hydrothermal fluids from sulfide chimneys; one area coincides with a sulfide mound, and the other is associated with a flat sediment surface. Unaltered hemipelagic sediment in Middle Valley consists of quartz, plagioclase, amphibole, smectite, chlorite, illite and irregular mixed-layer clays. Hydrothermally altered sediment additionally contains authigenic calcite (concretions and cement), barite, gypsum, pyrite, amorphous silica, and Mg-rich silicates. The altered sediment is enriched in Ca, Fe, S, Si, Cr and As; other elements such as Mn, Cu, Pb and Zn, which are concentrated in oxidized surface layers, were most likely enriched by diagenetic processes. Sulfides recovered in a core from the mound occur as alternating beds of coarse- and fine-grained clastic material of variable thickness, clast size, angularity and sorting, percentage and composition of non-sulfide matrix, and degree of oxidation. Sulfide minerals are pyrrhotite, pyrite, marcasite, sphalerite, isocubanite, chalcopyrite, covellite and galena. Non-sulfide phases are talc, barite, amorphous silica, Mg-rich clays, and iron oxides. Bulk chemical compositions indicate two types of mineralization in the core: type 1, which consists mostly of sulfide chimney clasts, has high Zn/Cu ratios, high Cd and Mo, and displays open interlocking networks of pyrrhotite laths infilled by sphalerite and Cu–Fe sulfides. Type 2, which forms veins that cut altered sediment, is enriched in isocubanite, As, Ag, Sb and Se. Values of $\delta^{34}S$ for sulfides are generally more positive than for sulfides formed in bare-ridge settings, and indicate that a significant component of the sulfur was derived from seawater sulfate abiotically reduced under hydrothermal conditions in the sedimentary pile. $\delta^{34}S$ values for pyrite, which are less than but track those for pyrrhotite, are consistent with textural relationships which show pyrite replaced pyrrhotite; $\delta^{34}S$ values of barite are less than for seawater, and indicate a large component of the sulfur formed from oxidized hydrothermal sulfur. Most of the sulfides in the mound core were precipitated initially either by quenching or mixing of hydrothermal fluids at or below the seafloor, and by replacement of earlier formed sulfides in chimneys during multiple hydrothermal events. Some of these sulfides have been redeposited as rubble mounds and stacked gravity flows which were later infilled and partly replaced by sulfides.

Keywords: seafloor, rift, hydrothermal, sulfides, hemipelagic, alteration, isotopes, mineralogy, chemistry, Juan de Fuca.

SOMMAIRE

«Middle Valley», vallée de rift délimitée par des failles et maintenant sédimentée, est située à l'extrémité septentrionale de la crête de Juan de Fuca. L'épaisseur de la couverture sédimentaire varie fortement, et augmente des bordures jusqu'à 1500 m au centre. Dans la vallée, huit monticules atteignant 60 m et d'un diamètre de plusieurs centaines de mètres, ont été étudiés par système d'imagerie acoustique (SeaMARC II) et relevé bathymétrique (Seabeam). Deux zones à flux de chaleur anormalement élevé correspondent à des zones de décharge hydrothermale. Dans un cas, il y a coïncidence avec un monticule de sulfures, tandis que l'autre est située dans un secteur sans relief. Le sédiment hémipélagique non altéré dans la vallée contient: quartz, plagioclase, amphibole, smectite, chlorite, illite, et argiles interstratifiées irrégulières. Là où il est altéré, le sédiment contient de plus, calcite authigène (sous forme de concrétions et de ciment), barytine, gypse, pyrite, silice amorphe, talc et silicates riches en Mg. Les roches altérées montrent un enrichissement en Ca, Fe, S, Si, Cr et As; d'autres éléments, tels que Mn, Cu, Pb et Zn, concentrés dans les niveaux oxydés à la surface, ont probablement été mobilisés par des processus diagénétiques. Les sulfures dans une carotte prélevée à proximité du monticule hydrothermal sont disposés en niveaux en alternance de débris clastiques à granulométrie fine ou grossière, dans lesquels l'épaisseur, la dimension des fragments, l'angularité, le granoclassement, la proportion et la composition de la matrice non sulfurée, et le degré d'oxydation sont variables. Les sulfures repérés sont: pyrrhotite, pyrite, marcasite, sphalérite, isocubanite, chalcopyrite, covellite et galène. Les composants non sulfurés comprennent: talc, barytine, silice amorphe, argiles magnésiennes, et oxydes de fer. Les compositions chimiques globales indiquent deux types de minéralisation; le premier, fait principalement de débris d'anciennes cheminées de sulfures, possède un rapport Zn/Cu élevé et une concentration de Cd et de Mo, et montre un réseau ouvert de lattes de pyrrhotite enchevêtrées, à remplissage de sphalérite et de sulfures de Cu–Fe. Le second occupe des fissures recoupant le sédiment qui sont enrichies en isocubanite, As, Ag, Sb et Se. Les valeurs de $\delta^{34}S$ des sulfures sont plus fortement positives, en général, que cel-

les des sulfures formés dans un milieu dépourvu d'une couverture sédimentaire. Elles indiquent qu'une partie importante du soufre est héritée du sulfate de l'eau de mer, réduit par processus abiotique dans l'amas de sédiments en milieu hydrothermal. Les valeurs de $\delta^{34}S$ de la pyrite sont décalées et plus faibles que celles de la pyrrhotite; cette relation concorde avec l'évidence texturale d'un remplacement de la pyrrhotite par la pyrite. Les valeurs de $\delta^{34}S$ de la barytine sont inférieures à celles de l'eau de mer, indiquant qu'une majeure partie de son soufre a été oxydé à partir du fluide hydrothermal. La plupart des sulfures prélevés à l'intérieur du monticule se sont formés à un stade initial, soit par trempe, soit par mélange des fluides hydrothermaux à l'orifice ou sous la surface, ce stade étant suivi de remplacements de sulfures précoces dans les parois des cheminées au cours des multiples événements hydrothermaux. Une partie des sulfures a été remobilisée et déposée sous forme d'amas de débris et d'empilement de coulées par gravité, les pores étant remplies et les sulfures remplacés en partie à un stade tardif.

Mots-clés: fond océanique, activité hydrothermale, sulfures, sédiment hémipélagique, altération, isotopes, minéralogie, chimie, crête Juan de Fuca.

INTRODUCTION

Few localities in the world's oceans are characterized by a spreading center overlain by a thick succession of hemipelagic and turbiditic sediments. In the NE Pacific, the Guaymas Basin is the best-studied. Here, hydrothermal deposits occur at the surface of a sedimentary sequence which has been altered by several thick doleritic sills and hydrothermal fluids (Lonsdale *et al.* 1980, Curray & Moore 1982). Within the sediment section, hydrothermal products include gypsum, smectite, and chlorite (Kastner 1982); sulfides at the seafloor are associated with barite, amorphous silica, stevensite and calcite (Peter 1986).

Sulfides occur in sediment-buried rifts in the Escanaba Trough of the South Gorda Ridge (Zierenberg *et al.* 1986), and in Middle Valley of the Northern Juan de Fuca Ridge (Fig. 1; Davis *et al.* 1987). Near the eastern margin of Middle Valley, an approximately north–south chain of eight mounds was detected with regional acoustic imagery (SeaMARC II), and subsequently with high-resolution SeaMARC I acoustic images and Seabeam bathymetry (Fig. 2; Davis *et al.* 1985, 1987). Detailed heat-flow transects of Middle Valley revealed two areas which displayed anomalously high heat flow. Area 1, at the southern margin of one mound (North Sulfide Mound), recorded heat-flow values of 1 to 1.3 W m^{-2} (Davis & Villinger, in prep.). Area 2 (Area of Active Venting), located 3 km NW of the Sulfide Mound, is a N–S lenticular belt of exceptionally high heat flow (up to 30 W m^{-2}) with no obvious mound-like structures (Fig. 2). In 1985, the North Sulfide Mound was photographed and 2.5 m of sulfide cored (Davis *et al.* 1987); hydrothermally altered sediment was recovered from the Area of Active Venting (Fig. 2). Of the 33 cores taken from Middle Valley during the PARIZEAU 85 cruise, one contains clastic sulfides, three have hydrothermally altered sediments, and the others consist of interbedded hemipelagic and turbiditic sediments. The recovery of both fresh and weathered clastic sulfides, and of hydrothermally altered sediment from Middle Valley has presented an excellent opportunity to study alteration assemblages associated with fluid–sediment reactions in the upflow zone of a hydrothermal system, hydrothermal minerals precipitated at and below the seafloor, and the effects of sedimentary reworking on sulfide distribution.

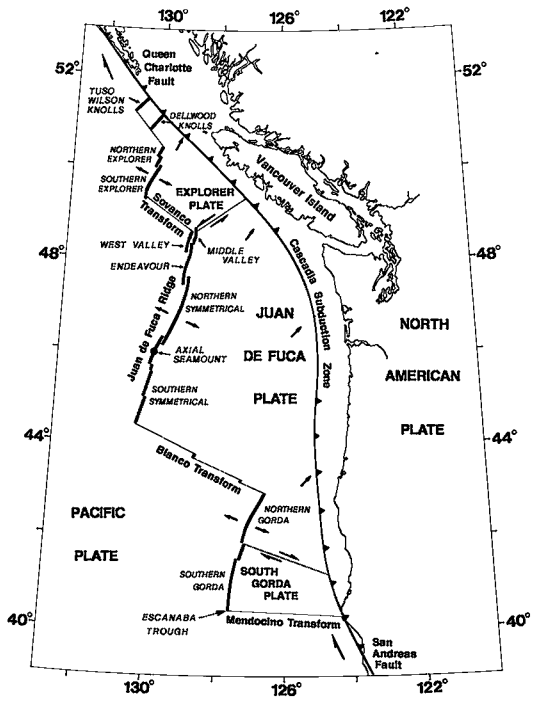

FIG. 1. Schematic map of the Juan de Fuca Ridge System showing the main tectonic elements and the location of Middle Valley.

GEOLOGICAL SETTING

The average half-spreading-rate of the Juan de Fuca Ridge is about 30 mm per year; morphology of the Ridge is similar to that of other medium- to fast-spreading centers where rifting occurs at the summit of a high-standing ridge. At a few localities such as Middle Valley, spreading took place in a depression due to slower spreading rates, proximity to a major transform fault, or lack of magma supply (Davis *et al.* 1987). During the Middle Brunhes Epoch, the spreading center in the Northern Juan

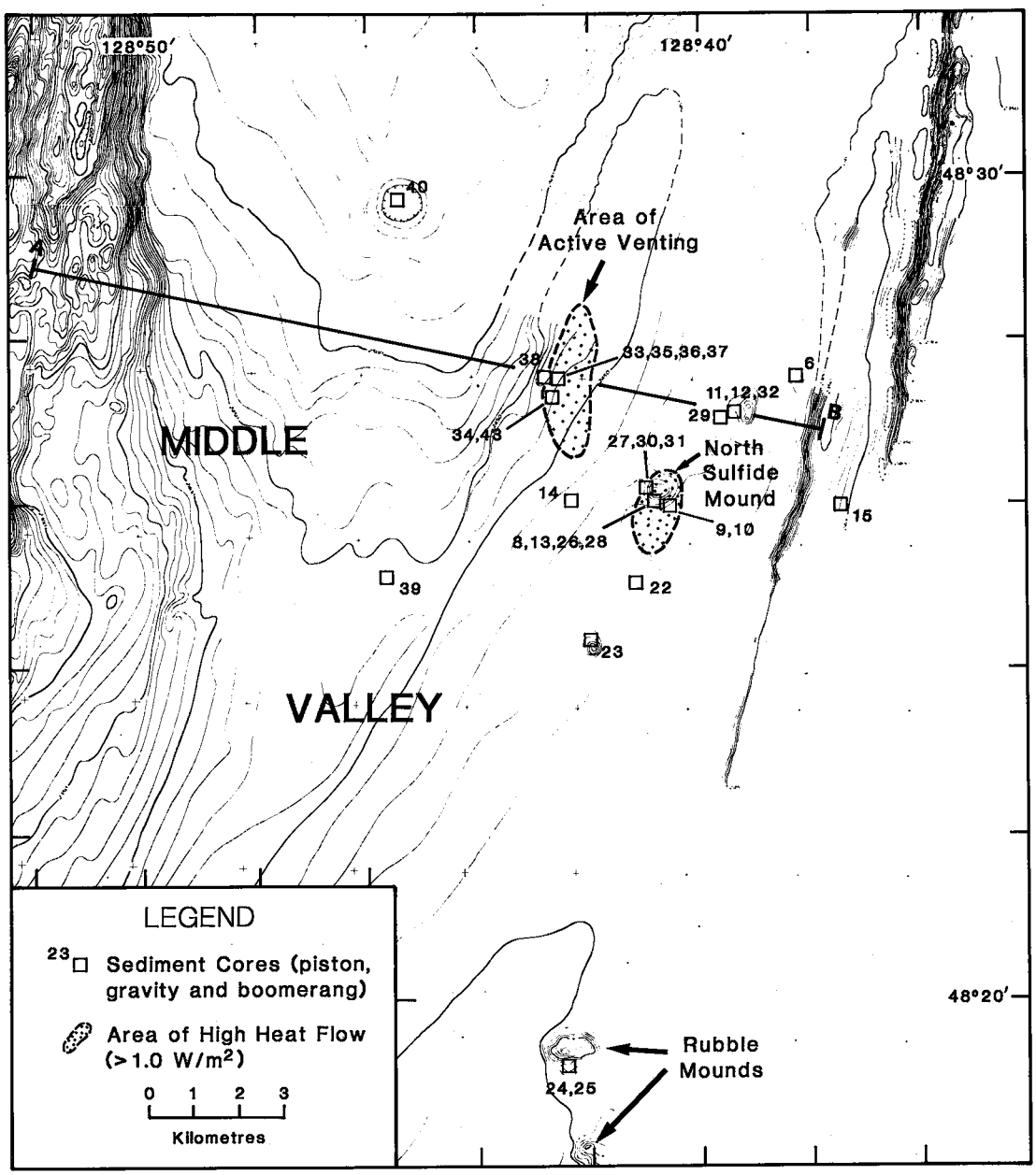

FIG. 2. Preliminary seabeam bathymetric map of Middle Valley (Davis & Sawyer 1987) showing the locations of sediment cores, heat-flow anomalies > 1 W m^{-2}, and the location of a seismic reflection profile (A–B) of Middle Valley. Heat-flow data from Davis & Villinger (in prep.).

de Fuca Ridge jumped westward to West Valley (Fig. 1; Davis & Lister 1977). Karsten *et al.* (1986) estimate this occurred during the last 200,000 years and probably as recently as the last few tens of thousands of years.

Because of its proximity to the continental margin, Middle Valley is filled by mostly terrigenous sediments. Seismic reflection profiles (Fig. 3) show the sedimentary sequence to consist of turbidite units of variable thickness interbedded with hemipelagic sediments, and to increase in thickness from the margins to the center of the basin, and from south to north. Sediment thicknesses range from ~300 m near the North Sulfide Mound to >1500 m near the

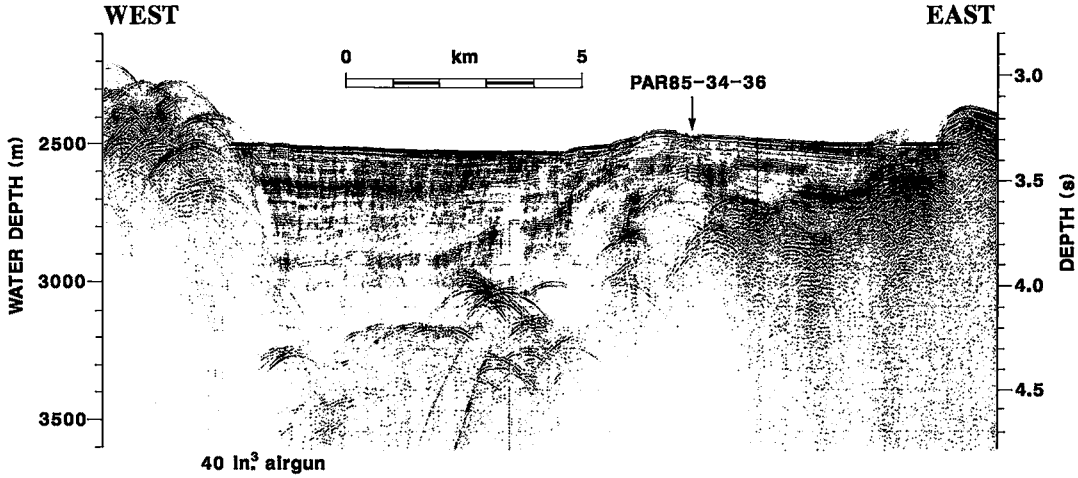

FIG. 3. West–east seismic reflection profile of Middle Valley at the location of cores PAR 85-34 and PAR 85-36 (refer to Fig. 2 for location).

northern boundary of Figure 2. Temperatures estimated for the base of the sedimentary pile range from 100°C near the fault-bounded margins to >300°C in a large area occupying the center of the basin (Davis & Lister 1977, Villinger & Davis 1986). This area has also been demagnetized, presumably by hydothermal alteration of magnetic minerals (Davis & Lister 1977). Elevated basement temperatures probably reflect the high thermal insulating capacity and low cross-stratal permeability of the sedimentary sequence, which would reduce conductive and convective heat loss from the lithosphere, respectively. The sedimentary pile plays an essential role, therefore, in maintaining high fluid temperatures and facilitating prolonged hydrothermal discharge at a restricted number of vent sites. Unlike sediment-barren ridges where the permeability is high and the lithosphere is cooled rapidly by widespread convection, the hydrothermal regime in Middle Valley is an energy-efficient one; this allows for the formation of large sulfide deposits at long-lived vent sites.

Mounds in Middle Valley have flat tops, are up to 60 m high and 1000 m across, and are transparent on both 3.5 kHz and seismic profiles (Fig. 3). The only internal features are strong discontinuous reflectors; a relatively weak surface reflector indicates that the mounds are now covered for the most part by a veneer of sediment (Davis *et al.* 1987). As Middle Valley has been tectonically, and therefore probably magmatically, inactive over the past 50,000 years, these reflectors most likely record layered sulfides rather than igneous sills within the mound.

Below the mounds and in the Area of Active Venting, the layering of turbiditic and hemipelagic sediment, which can be observed in 3.5 kHz echosounding and seismic profiles of Middle Valley (Fig. 3), is less distinct. This change in the acoustic properties of the sediments is probably due to pervasive hydrothermal alteration and sulfide precipitation in the upflow zone or saturation (or both) of the sedimentary pile with a gaseous phase such as methane and H_2S. Support for this interpretation is that sediment cored from the Area of Active Venting is hydrothermally altered, and contains high contents of methanogenic carbonate and H_2S.

SAMPLING AND ANALYTICAL METHODS

Cores of sediment were taken with boomerang, gravity, and piston corers. Core penetration ranged from 0.5 to 10 m. Samples of non-sulfidic sediment were first freeze-dried, and the sand and mud fractions were then separated using a 63-μm sieve. Grain-size analysis was performed using a Sedigraph 5000 D and a 2-m-long settling tube. The $CaCO_3$ fraction was removed and determined by HCl leaching. The clay fraction was analyzed on oriented slides using methods described by Chamley (1971) and Holtzapffel (1985).

Bulk geochemical analyses were performed at the Geological Survey of Canada Laboratories in Ottawa. Major-element oxides and Ba were determined by Inductive Coupled Plasma – Emission Spectrometry; Pb, As, Se, Cd and Sb were determined by Atomic Absorption Spectrometry; Cl and F were analyzed using anion chromatographic (Dionex) methods, and FeO, H_2O, S and CO_2 were determined by wet-chemical methods. Details of the analytical methods are given in Blaise & Bornhold (1987).

Samples for sulfur isotopic analysis were selected

from the least oxidized units of core PAR 85-13. Because of the fine grain size and intimate growth of several sulfide minerals, a combination of physical and chemical methods of mineral separation was used to obtain sulfur from sulfur-bearing phases. Clasts composed of one mineral (*e.g.*, pyrrhotite, barite) were sampled directly, whereas polysulfide clasts were crushed and ground, and sieved between 149 and 74 μm before separation into magnetic fractions using a Frantz Isodynamic Separator. Magnetic methods alone allow the concentration of pure pyrrhotite and pyrite. Concentrates consisting of two or more sulfur-bearing phases were then subjected to sequential chemical extraction. Mixtures of pyrrhotite, pyrite and barite were separated from sphalerite using magnetic methods, and pyrrhotite was preferentially dissolved in 6*M* HCl, and the H_2S liberated was precipitated as ZnS in zinc acetate solution. This precipitate was washed with hot deionized water into a beaker containing 25 ml of 0.1*M* $AgNO_3$ solution and the sulfide reprecipitated as Ag_2S. The residue from the above extraction was reacted with 1 g of $LiAlH_4$ in 50 ml of tetrahydrofuran to preferentially extract pyrite sulfur. The mixture was refluxed for 30 min. with increasing heat, and the reaction flask was then cooled in an ice-bath. After removal from the ice-bath, 50 ml of 6*M* HCl was added. The H_2S liberated was precipitated as Ag_2S. Finally, the sulfur bound in residual barite was reacted with Kiba reagent (Sasaki *et al.* 1979) at temperatures up to 300°C; H_2S was again precipitated in a zinc acetate solution as ZnS and then converted to Ag_2S.

$\delta^{34}S$ values were measured on a VG Micromass 602 mass spectrometer at the University of Ottawa. Results were standardized to Canyon Diablo troilite using the McMaster reference standards of Rees (1978). Analytical precision is $\pm 0.2‰$. Initial $^{87}Sr/^{86}Sr$ ratios were determined at Geochron Laboratories, Cambridge, Mass., U.S.A.; analytical precision is $\pm 0.1\%$.

Hemipelagic Sediment

Sedimentology

Core PAR 85-34 is representative of surficial hemipelagic and turbiditic sediments in Middle Valley. It can be divided into upper, middle and lower units (Fig. 4). The middle unit contains turbidites, generally below a 2-m depth in cores. The turbidite units contain detrital clays, quartz, amphibole and feldspar, and are almost free of biogenic components. The finest sediment, silty clay, consists of biogenic and terrigenous components. The average composition of hemipelagic intervals is given in Figure 5.

In sediment other than turbidites, the $CaCO_3$ content ranges between 5 and 30 wt.%. In the upper carbonate-rich beds, located at 75–77 cm and 160–

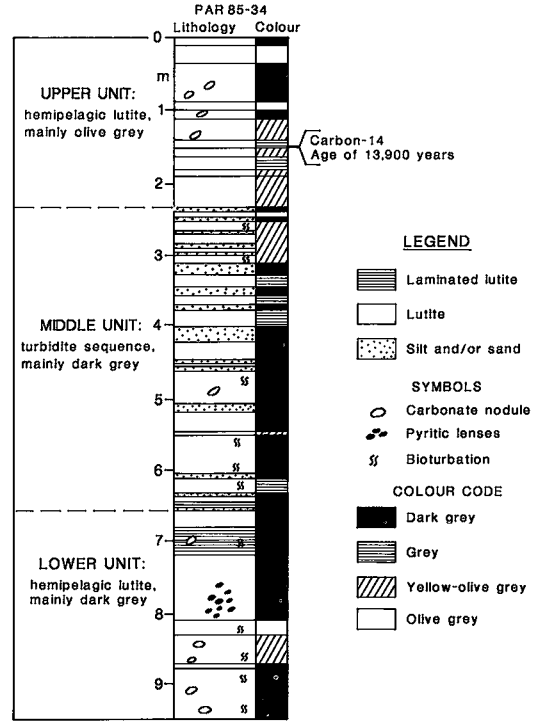

FIG. 4. Sedimentology of core PAR 85-34, Area of Active Venting, Middle Valley.

162 cm depth in PAR 85-28 and PAR 85-34, respectively, planktonic foraminifera (*globigerina bulloides*) have been ^{14}C dated at 13,490 (± 210) and 13,900 (± 180) years. Average sedimentation rates calculated using these dates for the top part of the sedimentary column are 5.5 – 5.8 cm Ka for core PAR 85-28, and 11.3 – 11.8 cm Ka for core PAR 85-34.

Mineralogy of unaltered sediment

Unaltered sediments in the study area are sedimentologically similar to hemipelagic and turbiditic sediments in the region of the Dellwood Knolls (Blaise *et al.* 1984, 1985, Blaise & Bornhold 1987). Bulk hemipelagic samples contain quartz, plagioclase, amphibole, mica and chlorite. The <2 μm fraction contains in decreasing order of abundance, smectite, chlorite, illite, and irregular mixed-layer clays with feldspar, amphibole and minor quartz (Fig. 5). Mineralogical variations of the clay fraction, although minor, are characterized by an increase in the ratio of primary (chlorite and illite) *versus* secondary (smectite and irregular mixed-layer) minerals during the Late Pleistocene compared to the Holocene. These changes result partly from continental weathering under different climatic conditions (Blaise *et al.* 1985, Blaise 1985).

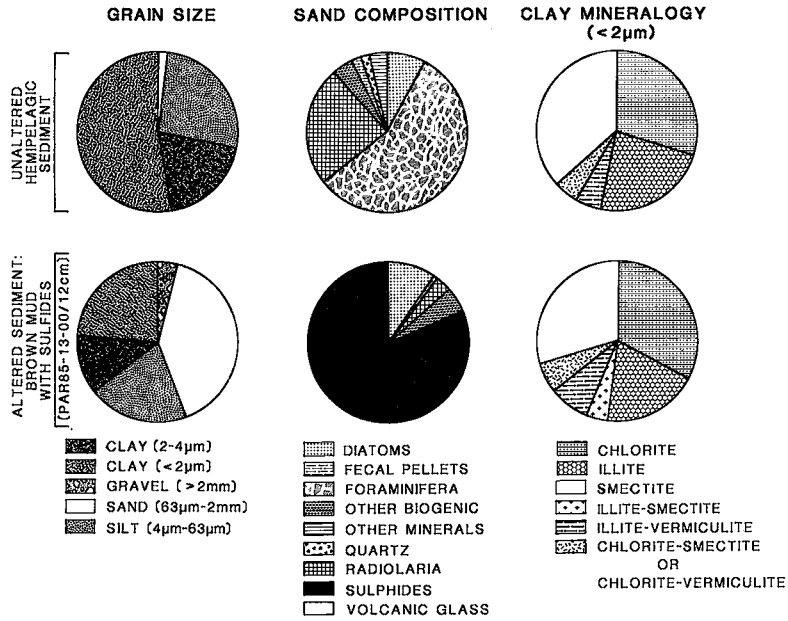

FIG. 5. Comparison of the grain size, sand composition and clay mineralogy for unaltered hemipelagic sediment, Dellwood Knolls (Blaise *et al.* 1984, 1985, Blaise & Bornhold 1987) and sulfidic sediment in core PAR 85-13, Middle Valley.

Mineralogy of altered sediment

Sediment in areas of high heat flow is slightly granular due to permeation by hydrothermal fluids. Carbonate concretions up to 5 cm in length occur in cores PAR 85-34 and PAR 85-36 (Fig. 6e), are greyish green and consist of terrigenous and biogenic clasts cemented by a fine-grained carbonate matrix. The biogenic clasts are partly to totally replaced by fine-grained calcite. Pyrite and barite occur in carbonate nodules in the top sections of core PAR 85-34, and in core PAR 85-36. In cores PAR 85-28 and PAR 85-34, the sand fraction contains barite, gypsum, Mg-rich silicates and pyrite cubes, which do not occur in other PARIZEAU cores of the area. Sheafs of euhedral gypsum (Fig. 6c,h,i) also occur. Gypsum is most common below depths of 840 cm in PAR 85-34, and is commonly associated with framboidal pyrite (Fig. 6c,h). Barite forms rosettes (Fig. 6a,b), many which are associated with cubic pyrite (Fig. 6d,f,g). Throughout the entire core, the sediment is partly cemented by calcite and amorphous silica (Fig. 6j); silica also replaced worm tubes and foraminifera.

Geochemistry

In cores PAR 85-27 and PAR 85-36, the contents of Al, total Fe, K, P, Ti, Be, La, V and Yb increase with depth, whereas Na, Mg, Mn, Ba, Cu, Ni, Pb, Sr and Zn display inverse trends (Fig. 7). In core PAR 85-34, the geochemical variations are clearly related to the three units shown in Figure 4. The middle unit, which is composed mostly of turbiditic sediments, is rich in lithophile elements Al, K, P, Ti, Be, La, V and Yb. Fine-grained upper and lower units which are composed of hemipelagic sediment display inverse trends for these elements; Ca, Fe^{3+}, Fe^{2+}, S, Si, Cr and As are often anomalously high. The enrichment of most of these elements probably reflects the formation of authigenic minerals from hydrothermal fluids. Elements concentrated in surface samples, such as Mn, Cu, Pb and Zn, were most likely enriched by diagenetic processes.

The element contents of hydrothermally altered sediment from PAR 85-27, PAR 85-34 and PAR 85-13, and unaltered hemipelagic sediment from PAR 85-31 and PAR 85-39 (Reference Hemipelagic Sediment, R.H.S.) are compared in Figure 8. Elements enriched in all three hydrothermally altered cores include Fe, Mn, S, Cu, Zn and Pb; Mg and As, and Sr and As have elevated contents in PAR 85-13 and PAR 85-34, respectively. Most lithophile-element decreases, particularly in PAR 85-13, are due to the dilution effect of high sulfide contents, except Fe^{2+} and Ca in PAR 85-27 and PAR 85-34, and Ca in PAR 85-13.

The $\delta^{13}C$ and $\delta^{18}O$ values in carbonate nodules from core PAR 85-34 range from −38 to −12‰, and −11.1 and +4.3‰, respectively. There is a general trend of increasing $\delta^{13}C$ and decreasing $\delta^{18}O$ values

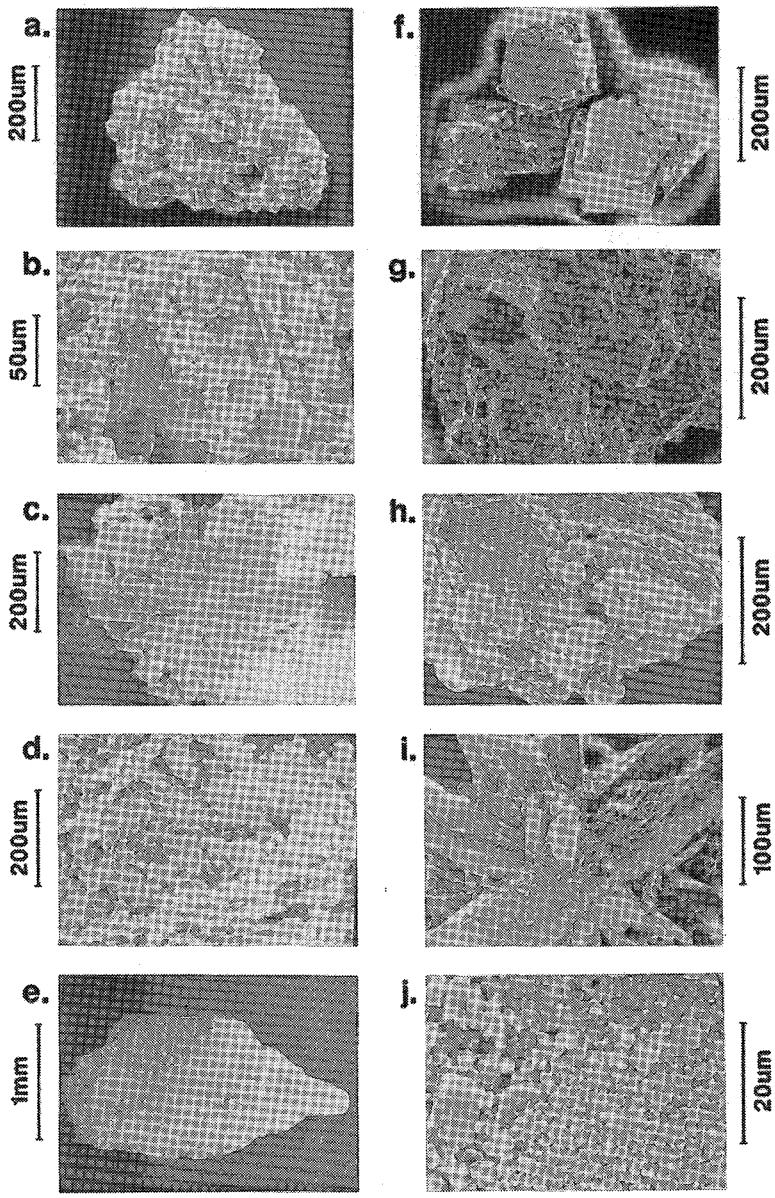

FIG. 6. Scanning electron microphotographs (SEM) of hydrothermal mineral assemblages in cores PAR 85-34 and PAR 85-28, Middle Valley. (a) Barite with radial habit, core PAR 85-28, 410–412 cm. (b) Barite rosette; same core interval as (a). (c) Gypsum with pyrite framboids on surfaces, core PAR 85-34, 840–842 cm. (d) Cubes and framboids of pyrite intergrown with authigenic talc and montmorillonite-group minerals; same core interval as (c). (e) Carbonate concretion that replaced foraminifera, core PAR 85-34, 110–112 cm. (f) Aggregate of pyrite cubes, core PAR 85-34, 180–182 cm. (g) Pyrite cubes in sediment, core PAR 85-34, 920–922 cm. (h) Framboids of pyrite on authigenic euhedral gypsum crystals, core PAR 85-34, 920–922 cm. (i) Prisms of authigenic euhedral gypsum, PAR 85-34, 922–926 cm; fine-grained crystals are also gypsum. (j) Turbiditic sediment cemented with calcite, core PAR 85-34, 900–902 cm.

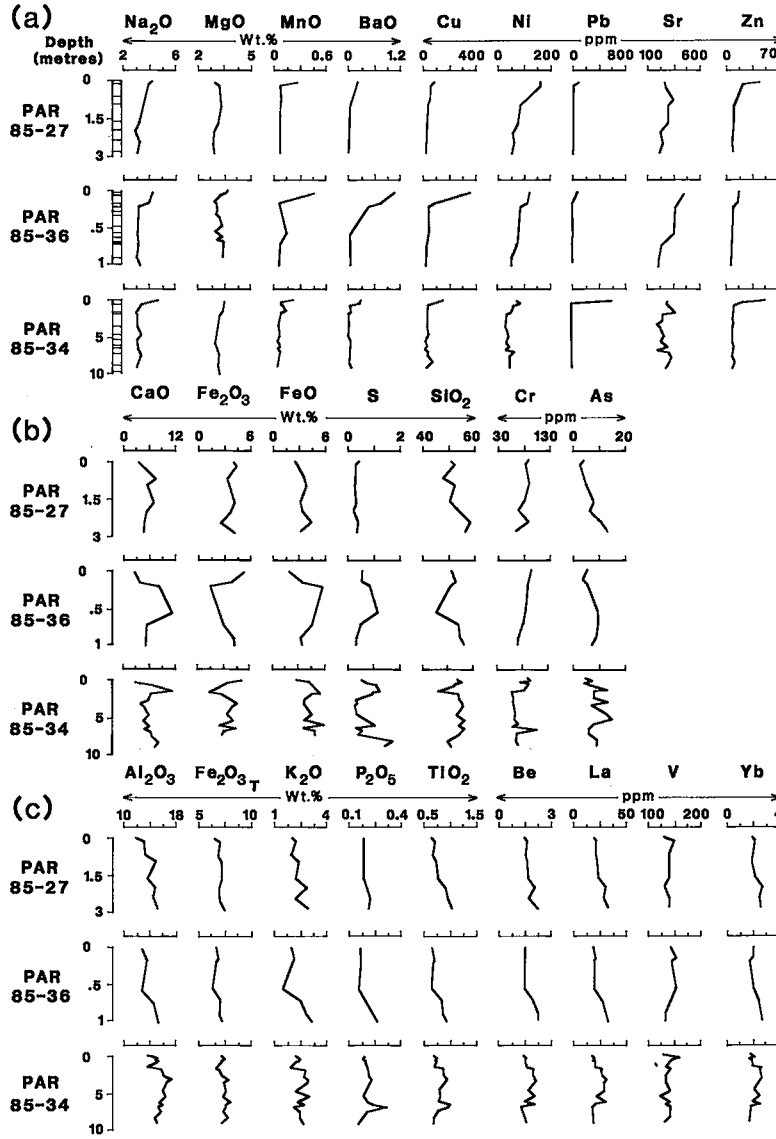

FIG. 7. Chemical variations in bulk sediment for cores PAR 85-34, PAR 85-27 and PAR 85-36, as a function of depth below the seafloor: (a) elements accumulated by diagenetic or hydrothermal (or both) plume processes at the surface; (b) elements which display local anomalies due to hydrothermal processes; and (c) elements associated with Pleistocene turbiditic deposits.

with depth. Calcite from some nodules with highly negative $\delta^{13}C$ values was probably derived from carbonate formed by microbial methane oxidation, whereas less negative $\delta^{13}C$ values represent a mixture of methanogenic and seawater carbon (Al-aasm & Blaise 1987). This interpretation is supported by the inverse relationship between $\delta^{13}C$ and $\delta^{18}O$ values; as $\delta^{13}C$ values become less negative, $\delta^{18}O$ values become more negative, indicating higher paleotemperatures and therefore a larger hydrothermal fluid component with depth. Maximum temperatures calculated on the basis of oxygen isotope fractionation between calcite and 0.0‰ seawater are in the order of 70°C (Al-aasm & Blaise 1987).

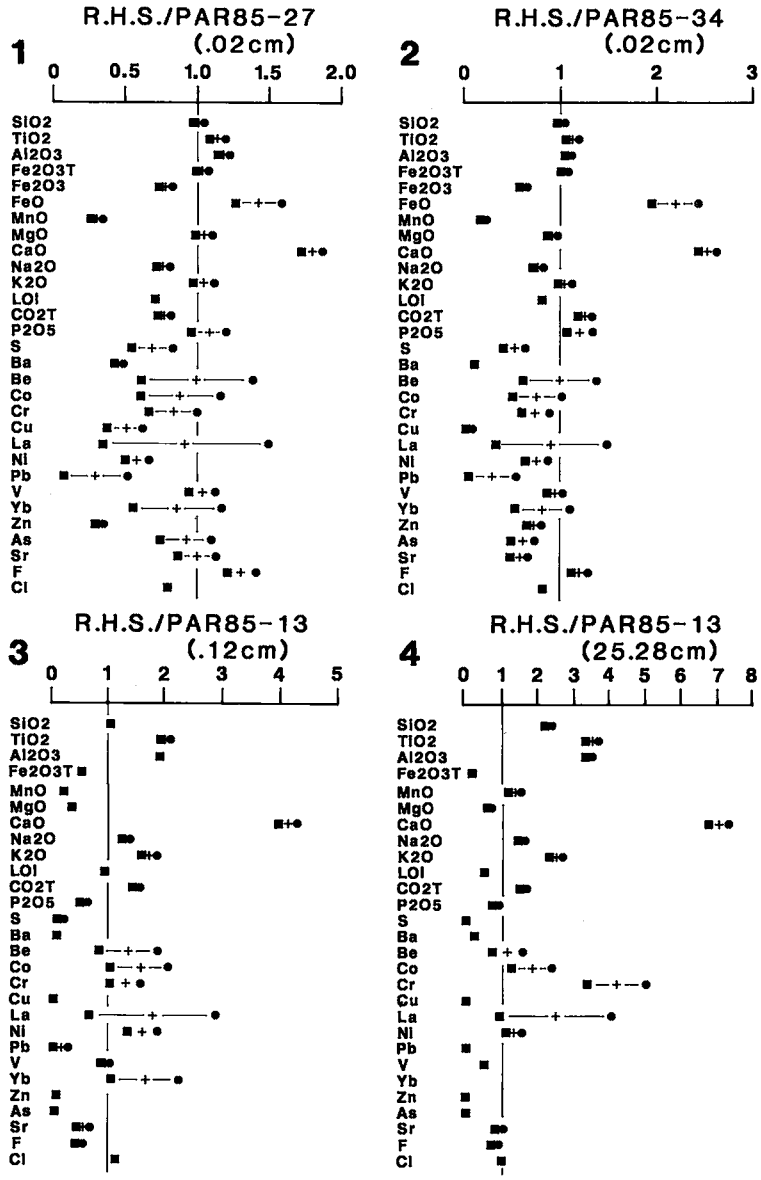

FIG. 8. Plots of ratios of element contents of reference hemipelagic sediment (R.H.S.) and element abundances in cores PAR 85-27, 85-34 and 85-13. In the case of core PAR 85-13, comparisons were made for both brown mud at the surface and black sulfidic mud 25–28 cm below the surface. Symbols: + = $\text{mean}_{\text{R.H.S.}}/\text{mean}_{\text{sample}}$; solid square = $\text{mean}_{\text{R.H.S.}}$ − (standard deviation/$\text{mean}_{\text{sample}}$); solid circle = $\text{mean}_{\text{R.H.S.}}$ + (standard deviation/$\text{mean}_{\text{sample}}$).

Values of $\delta^{34}S$ in pyrite from PAR 85-34 range between −39.7‰ and −12.8‰; $\delta^{34}S$ values for gypsum approach seawater values (Fig. 14). $\delta^{34}S$ values less than −30‰ are within the range of sulfides formed by bacterial sulfate reduction under open marine conditions (Goldhaber & Kaplan 1974). $\delta^{34}S$ values greater than −15‰ may reflect sulfate reduction under partly closed conditions, or the influx of isotopically heavy hydrothermal sulfur. The association of these values with pyrite cubes, higher temperatures estimated from $\delta^{18}O$ values in calcite concretions, and positive $\delta^{34}S$ values in massive sulfides

from the North Sulfide Mound, are consistent with a hydrothermal sulfur component.

Gypsum from the top of PAR 85-43 has a $^{87}Sr/^{86}Sr$ ratio of 0.70665. This value, which falls between the ratio for seawater (0.7091, Burke *et al.* 1982) and deep-sea basalt (0.7029, Subbarao & Hedge 1973, O'Nions & Pankhurst 1973) indicates that a component of the Sr in gypsum was derived from a primitive, presumably basaltic, source.

Hydrothermal Sediment

Sedimentology and textural relationships

Core PAR 85-13 from the southern flank of the North Sulfide Mound penetrated 2.35 m of weakly consolidated massive to semi-massive sulfides capped by 20 cm of brown oxidized sediment (Figs. 2, 11). Alternating beds of coarse- and fine-grained clastic sulfides display variable thickness, clast size and sorting, percentage and composition of non-sulfidic matrix, and degree of oxidation.

The coarse-grained sulfide units (Fig. 9a) can be either clast- or matrix-supported. Sulfide clasts range in diameter from <1 mm to >8 cm, are generally sub-rounded to angular, are poorly sorted except in one unit where the sulfide grains appear graded, and are highly variable in texture and composition. One clast consists of pyrrhotite crystals oriented radially about a chimney orifice; other clasts display concentric growth patterns. Most sulfide clasts have textures similar to those described for chimneys. Most clasts are composed of pyrrhotite and pyrite with minor sphalerite and Cu sulfides; some clasts are mainly sphalerite. Non-sulfide clasts consist of soft and deformed hemipelagic sediment, barite, talc, and basaltic glass altered to palagonite. Some hemipelagic sediment clasts are rimmed by pyrite (Fig. 10f). The sulfide component within coarse-grained clastic units rarely exceeds 80 wt.%.

The finer grained sulfide units (Fig. 9b) are composed of single or composite grains in a matrix of altered hemipelagic sediment, Mg-rich silicates, and palagonite. These units, which contain up to 70 wt.% sulfides, contain more talc and palagonite than the coarser grained hydrothermal sediment. Veinlets of Fe oxides cut the finer grained sediments in places (Fig. 9b).

Mineralogy

The sulfide minerals in core PAR 85-13 in order of decreasing abundance are pyrrhotite, pyrite, sphalerite, marcasite, isocubanite, chalcopyrite, covellite and galena. Non-sulfide phases are talc, Mg-rich clays, amorphous silica and barite. Oxidation products of Fe sulfides are hematite, magnetite, lepidocrocite and goethite.

Pyrrhotite occurs most commonly as an open interlocking network of hexagonal plates (Fig. 9c,d) up to several mm in length which is partly infilled by black, commonly hexagonal-shaped Fe-rich sphalerite (Fig. 9f,g). The hexagonal outline of zinc sulfide grains indicate they were originally wurtzite and have inverted to sphalerite during cooling. Isocubanite with exsolution-like lamellae of chalcopyrite distributed along its crystallographic axis (Fig. 9h) occurs within sphalerite. Chalcopyrite also occurs as a replacement rim around isocubanite. The pyrrhotite is rimmed and replaced to variable degrees by pyrite (Fig. 10d) and less commonly marcasite (Fig. 10b). In some samples, pyrrhotite laths are entirely replaced by pyrite grains, producing a lacy texture (Fig. 10a) in which the interstices are filled with pyrite. Pyrite also rims ragged clasts of hemipelagic sediment (Fig. 10f). Galena cubes are rarely present in marcasite (Fig. 10b).

Barite generally occurs as authigenic rosettes (Fig. 10h; see also Davis *et al.* 1987) in a matrix of altered hemipelagic sediment formed most likely by the reaction of hydrothermal fluids with hemipelagic sediment. Barite also occurs as subhedral grains within the interstices of some sulfide clasts, and as intergrowths with silica and pyrite in others. Mg-rich silicates form fibrous masses (Fig. 10g) commonly associated with barite.

Individual barite crystals from various depths in the core have average SrO contents ranging from

FIG. 9. (a) Polished slab of epoxy-impregnated sulfides from core PAR 85-13 (85–90 cm depth) showing reworked nature of clastic sulfides (dark grey). Light grey clasts are talc and barite. (b) Polished slab of epoxy-impregnated sulfidic mud from core PAR 85-13 (54–60 cm depth) showing cross-cutting veins and associated alteration aureoles. (c) SEM secondary electron image showing open, interlocking hexagonal pyrrhotite crystals. Core PAR 85-13. (d) SEM secondary electron image of hexagonal pyrrhotite crystals encrusted by pyrite. Core PAR 85-13. (e) SEM secondary electron image of pyrite cubes which have grown in the interstices of a pyrrhotite network. Core PAR 85-13. (f) Photomicrograph showing the open interlocking network of pyrrhotite (po) tablets which are partly replaced by Fe oxide, and infilled by sphalerite (sp) with central accumulations of isocubanite (ISS) and chalcopyrite (cp). Reflected light. Dredge sample MV.DR.06.08 from North Sulfide Mound. (g) Photomicrograph of sphalerite (sp) from same sample as in (f) showing hexagonal outline and central accumulations of Cu–Fe sulfides (ISS/cp). Reflected light. (h) Photomicrograph of Cu–Fe sulfides showing lamellae of chalcopyrite (cp) oriented along isocubanite (ISS) crystallographic axis. Reflected light. Core PAR 85-13, 97–99 cm.

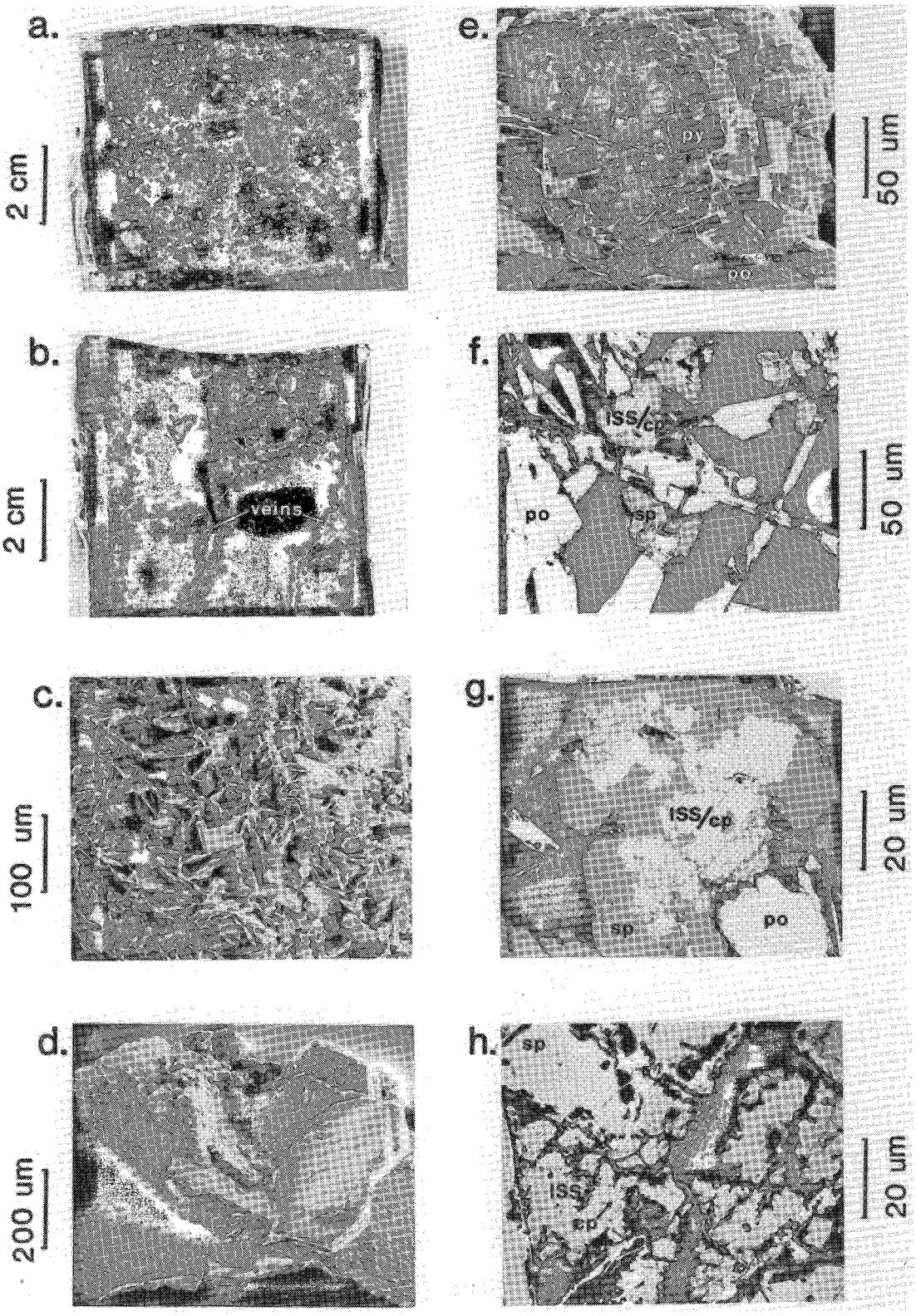
a.
2 cm
b.
2 cm
veins
c.
100 um
d.
200 um
e.
py
po
50 um
f.
iss/cp
po
sp
50 um
g.
iss/cp
sp
po
20 um
h.
sp
iss
cp
20 um

TABLE 1. STRONTIUM CONTENT OF BARITE FROM CORE PAR 85-13, MIDDLE VALLEY, DETERMINED BY MICROPROBE METHODS

		SrO wt.%			
Core Number	Range (cm)	Average	Min.	Max.	Number
PAR 85-13	45-48	2.53	1.71	3.60	5
	54-60	3.76	0.97	5.97	5
	85-90	1.82	1.00	2.84	4
	96-102	2.93	0.71	7.91	5
	110-117.5	5.43	1.19	11.63	6
	135-140	1.05	0.86	1.31	4
	190-197	3.25	1.10	5.94	5
	207-214	3.04	2.55	3.31	4
PAR 85-13	232-237.5	1.78	1.65	2.03	4

TABLE 2. CHEMICAL COMPOSITION OF 43 SAMPLES FROM CORE PAR 85-13, JUAN DE FUCA RIDGE

Element Oxides (wt.%)							
	X	Min.	Max.		X	Min.	Max.
SiO_2	17.40	5.60	48.90	CaO	0.45	0.16	1.47
Al_2O_3	2.96	0.46	12.00	MgO	4.84	2.43	13.40
K_2O	0.39	0.10	1.41	MnO	0.12	0.04	0.40
Na_2O	1.26	0.41	3.86	TiO_2	0.10	0.01	0.49
				P_2O_5	0.15	0.05	0.69
Elements (ppm)							
Fe (total)(%)	30.3	8.20	42.1	Sb	26.9	4.60	60.1
S (total)(%)	26.0	0.53	37.7	Mo	108	8.20	188
Ba(%)	1.97	0.42	5.06	Ni	95	61	285
Cu	0.40	0.06	1.11	Co	25	17	32
Zn	2.47	0.06	4.40	Bi	0.61	0.50	1.30
Pb	0.04	0.015	0.094	W	4.56	4.00	17.0
Ag	8.70	0.20	21.8	Be	0.45	0.10	1.30
Cd	39.5	0.70	88.6	B	34.0	5.60	153
As	227	54	454	La	6.10	1.00	29.00
Se	87.7	7.90	267	Yb	4.50	2.60	5.60
				V	151	79	357

X = mean value

1.05 to 5.43 wt.% (Table 1). Although individual barite grains contain as much as 11.63 wt.% SrO, a separate strontium mineral such as celestite was not detected.

Oxidation is most pronounced in the upper 80 cm of the core where entire clasts of pyrrhotite have been completely replaced by Fe oxides (Fig. 10c), indicating that some of their oxidation took place after deposition as clastic sediments. In some clasts, pyrrhotite cores are replaced by multiple layers of concentrically zoned lepidocrocite (Fig. 10d,e).

Geochemistry

Bulk chemistry. Average values and ranges of major and trace elements in PAR 85-13 are given in Table 2; raw values are plotted in Figure 11. The concentrations of most chalcophile elements, *e.g.*, Fe, Zn, Cd, As, Sb, Mo and Se, are a function of the total sulfide content, particularly below 80 cm where the sulfides are less oxidized and the content of hemipelagic sediment is lower. Sulfides within core PAR 85-13 can be classified into two types on the basis of geochemistry (Fig. 12). Type 1 sulfides, which occur between 80 and 240 cm, are characterized by high Zn/Cu ratios, by high contents of Cd (bound in sphalerite), and by lower contents of As, Sb and Se. Type 2 sulfides, which are restricted to a zone hosted by altered hemipelagic sediment between 20 to 60 cm in depth, consist of isocubanite and less common chalcopyrite, and are characterized by high Cu/Zn ratios and high contents of As, Sb, Ag and Se. In some samples, veinlets of isocubanite cross-cut altered sediment.

In the top 20 cm of core, Mn, Ba, Zn, Fe, Mg, P, S, Pb, As, Sr, F and Cu are enriched relative to hemipelagic sediment (Fig. 8). The Mn may have originated from hydrothermal plumes known to be active in Middle Valley (Baker *et al.* 1987); alternatively, Mn may have been dissolved under reducing conditions in the subsurface, and precipitated in the zone of oxidation just below the sediment–seawater interface.

The hydrothermal components in core PAR 85-13 consist of a mixture of resedimented chimney sulfides and non-sulfides (*e.g.*, Mg-rich silicates, barite) derived from hydrothermally altered sediment. On a SiO_2–MgO–S ternary diagram (Fig. 13), samples from sulfide-rich units in core PAR 85-13 plot on or near a line between talc and massive sulfide. Samples from finer grained units in PAR 85-13, which contain a greater proportion of Mg-rich silicates or hemipelagic sediment (or both), plot between this mixing line and unaltered hemipelagic sediment from Middle Valley (Fig. 13).

FIG. 10. (a) Photomicrograph of lacy subhedral pyrite (py) which infilled pyrrhotite network and partly replaced pyrrhotite. Minor sphalerite (sp). Reflected light. Core PAR 85-13, 96–102 cm depth. (b) Photomicrograph showing galena (gn) in marcasite (m) which replaced pyrrhotite (po) and pyrite (py). Sphalerite (sp) with central accumulations of chalcopyrite (cp) occurs in the interstices of the Fe sulfide network. Reflected light. Core PAR 85-13, 122–123 cm. (c) Photomicrograph of pyrrhotite network completely replaced by Fe oxides. Pyrite (py) occurs in the interstices. Reflected light. Dredge sample MV.DR.06.02B, North Sulfide Mound. (d) Photomicrograph of network of pyrrhotite grains, each rimmed by pyrite (py) and replaced by successive bands of Fe oxides. Reflected light. Dredge sample MV.DR.06.03, North Sulfide Mound. (e) Closeup of (d) showing the concentric zonation of Fe oxides (mostly lepidocrocite) which replaced the core of a pyrrhotite crystal. Reflected light. Dredge sample MV.DR.06.03, North Sulfide Mound. (f) Photomicrograph of clasts of hemipelagic sediment which have been rimmed by pyrite, following sedimentation. Reflected light. Core PAR 85-13, 97–144 cm. (g) SEM backscatter electron image showing a fibrous matt of Mg-rich silicates between sulfide grains. Core PAR 85-13, 85–90 cm. (h) Photomicrograph of barite rosette hosted in sulfides. Reflected and transmitted light. Core PAR 85-13, 232–237 cm.

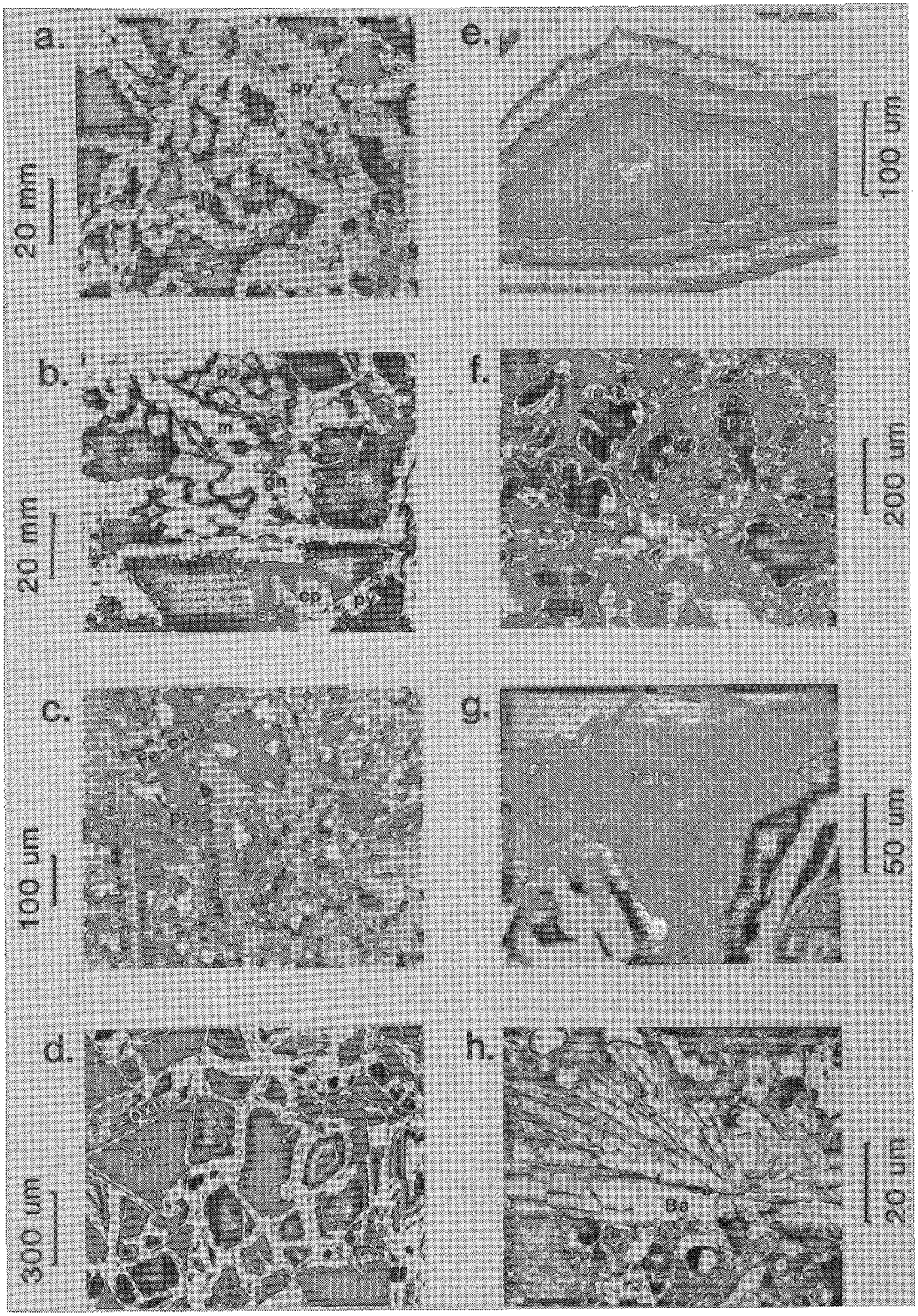
a.
20 mm
pv
b.
20 mm
po
m
dn
cp
py
c.
100 um
Foraminifera
d.
300 um
e.
100 um
f.
200 um
g.
50 um
Valve
h.
20 um
Ba

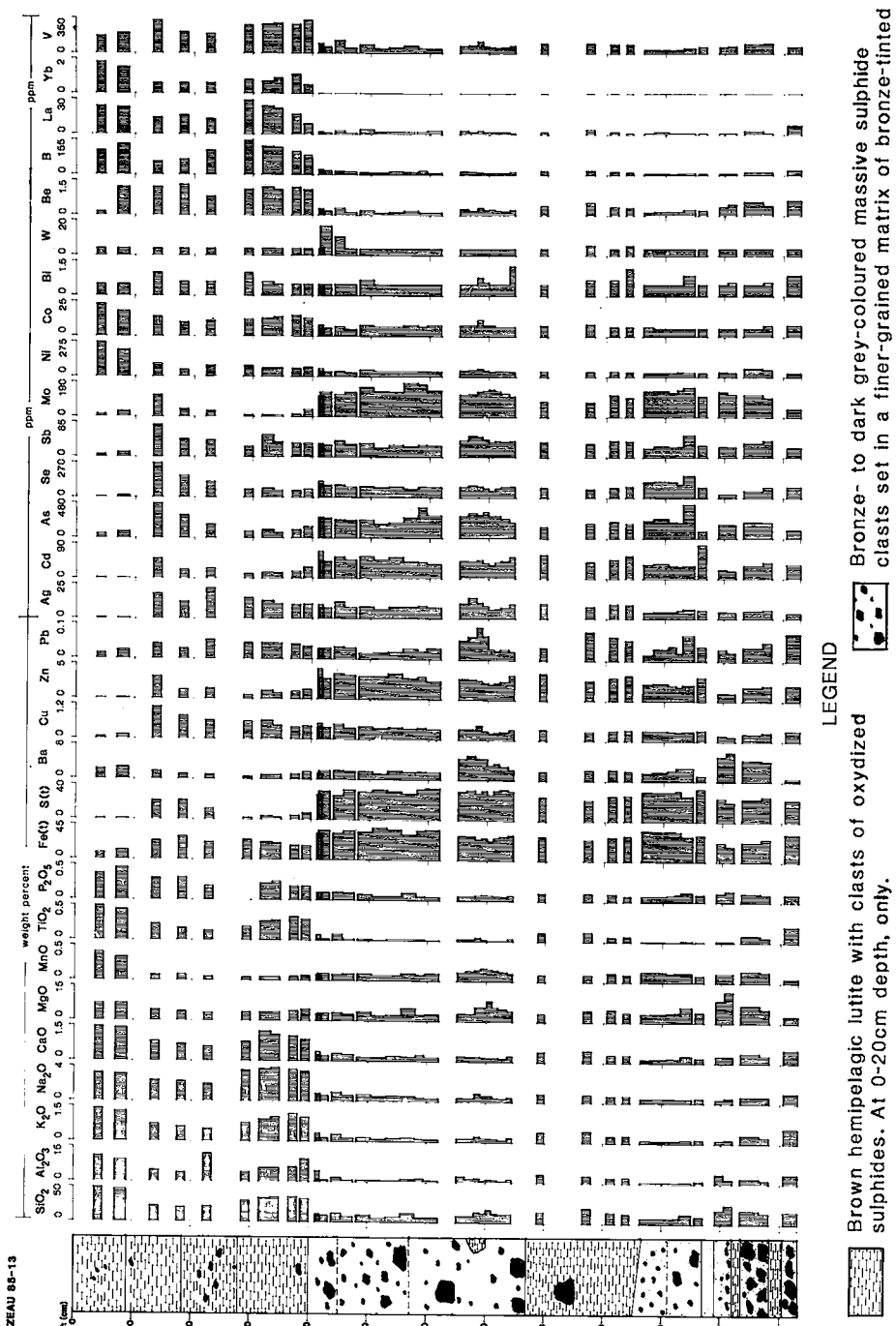

FIG. 11. Sedimentological log and geochemical profiles for bulk samples from core PAR 85-13.

Sulfur isotopes. The frequency distribution of $\delta^{34}S$ values in pyrrhotite, pyrite, barite and gypsum from Middle Valley, and in sulfides from the East Pacific Rise and Juan de Fuca Ridge, are presented in Figure 14. The $\delta^{34}S$ values in pyrrhotite and pyrite are positive and highly variable, ranging up to 17.6 and 14.7‰, respectively, and plot between values for oceanic basalts (Sakai *et al.* 1984) and seawater. These values are consistently more positive than $\delta^{34}S$ values for sulfides from sediment-barren ocean ridges (Fig. 14; Styrt *et al.* 1981, Arnold & Sheppard 1981, Kerridge *et al.* 1983, Shanks & Seyfried 1987). Barite displays a narrower range of values and averages 10.1‰.

Highly positive values for sulfides from Middle Valley can best be explained by contamination of primitive sulfur, leached from the underlying basaltic crust, with isotopically heavier sulfur. The most probable source of this sulfur is sulfide generated under hydrothermal conditions in the sedimentary column by abiotic reduction of sulfate during reaction with organic matter. This reaction has been shown to be important at temperatures greater than 250°C (Kiyosu 1980). The sulfate was probably derived from seawater trapped in permeable turbidite units during sedimentation, or recharged into permeable units by hydrothermal convection. Increasing heat flow from the margins to the center of the basin indicates that some recharge is taking place, although how much of this occurs within the sedimentary pile is unknown.

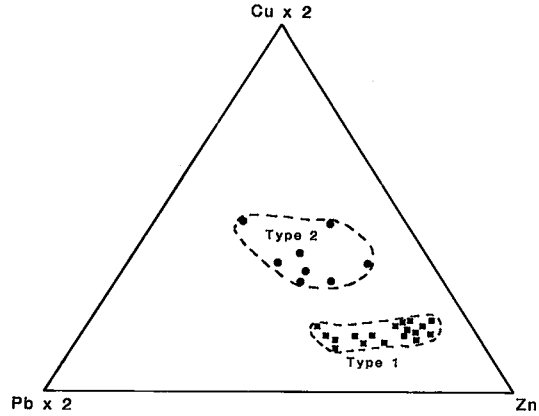

FIG. 12. Ternary Pb–Zn–Cu plot of sulfidic sediments from core PAR 85-13 showing the chemical differences between "feeder" (Type 1) and chimney (Type 2) sulfides, Middle Valley.

The $\delta^{34}S$ values for coexisting pyrite and pyrrhotite track each other, but values for pyrite are consistently less than those of pyrrhotite. These sulfides are clearly not in isotopic equilibrium; the order of $\delta^{34}S$ enrichment determined experimentally under equilibrium conditions places pyrite > pyrrhotite (Kajiwara & Krouse 1971). The tracking of $\delta^{34}S$ values in pyrite and pyrrhotite indicates that most of the pyrite sulfur was derived from coexisting pyrr-

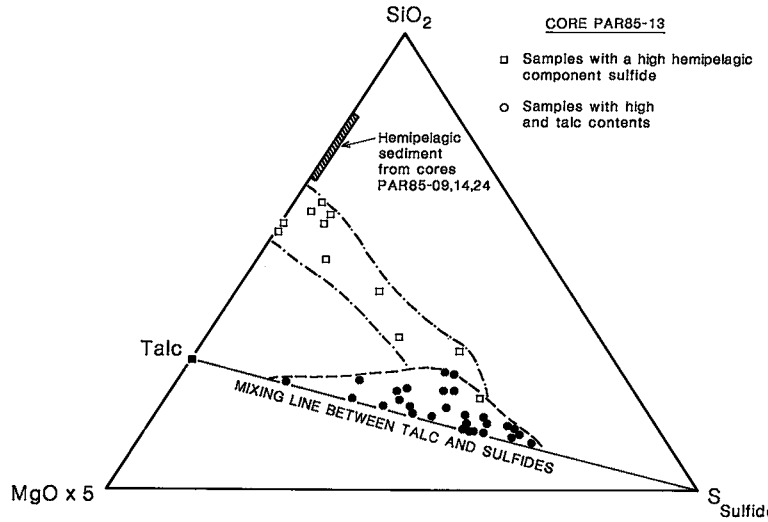

FIG. 13. Ternary SiO_2–MgO–S plot of samples from PAR 85-13 (mostly sulfidic sediment) and cores PAR 85-09, PAR 85-14 and PAR 85-24 (unaltered hemipelagic sediment). Most samples from PAR 85-13 plot either on a mixing line between sulfides and talc, or between this mixing line and unaltered hemipelagic sediment.

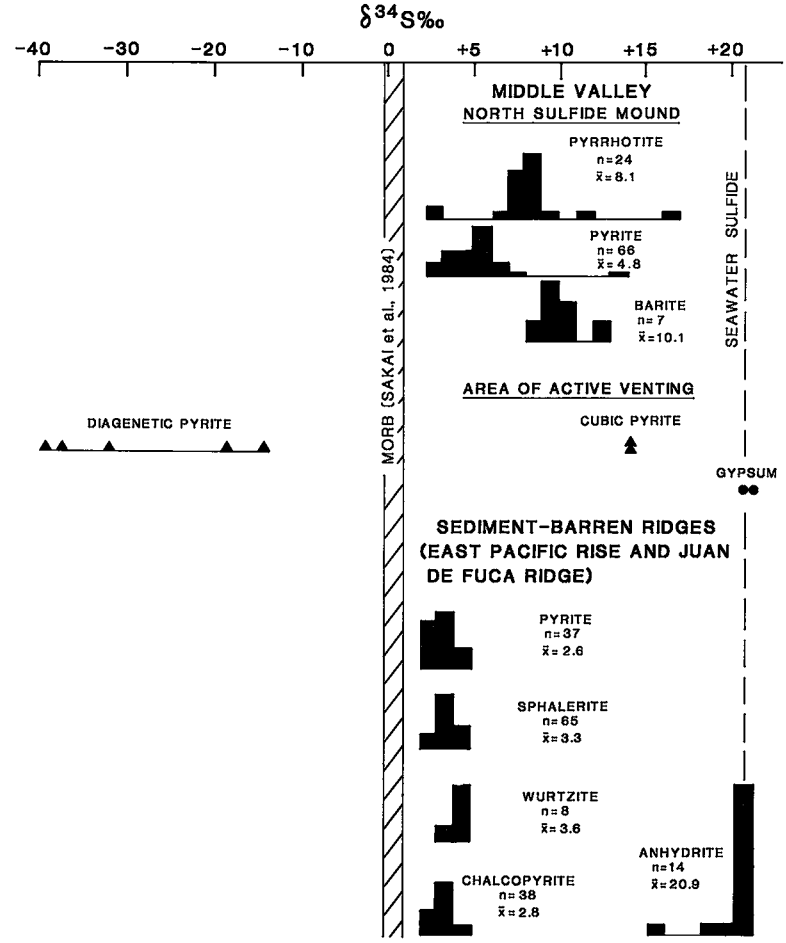

FIG. 14. Histograms of $\delta^{34}S$ values for pyrrhotite, pyrite and barite from the North Sulfide Mound, and pyrite and gypsum from the Area of Active Venting. Also plotted are histograms of $\delta^{34}S$ values in pyrite, wurtzite, sphalerite, chalcopyrite and anhydrite from the sediment-barren East Pacific Rise and Juan de Fuca Ridge (from Styrt *et al.* 1981, Arnold & Sheppard 1981, Kerridge *et al.* 1983, Shanks & Seyfried 1987), and the range of $\delta^{34}S$ values in oceanic basalts (Sakai *et al.* 1984) and seawater.

hotite. This is consistent with the mineral paragenesis which shows pyrite replaced pyrrhotite. Given that pyrrhotite in clasts originated in chimneys, the later precipitation of pyrite may reflect entrainment of seawater into the chimneys. This would simultaneously decrease the temperature and increase the oxygen fugacity, both of which would favor pyrite precipitation.

Values of $\delta^{34}S$ in barite are considerably less positive than seawater sulfate. This suggests that a significant proportion of the sulfur in barite originated from the oxidation of dissolved H_2S or precipitated sulfide.

DISCUSSION

Hemipelagic sediment

Hemipelagic sediment from Middle Valley consists of continental, marine, diagenetic and hydrothermal components. During the Late Pleistocene glaciation, the amount of terrigenous material deposited in deep-sea environments was greater than at present (McCoy & Sancetta 1985, Blaise *et al.* 1988). Because the sediment originated mainly by mechanical erosion associated with ice movement, the chemical composition reflects that of the source rocks (Barron &

Whitman 1981). As a result, the geochemical relations among lithophile elements in the hemipelagic sediments (Si, Al, K, P, Ti, Fe^{3+}, Be and Yb) should reflect element associations in the average source terrains.

The marine component of these sediments is mostly biogenic carbonate and amorphous silica. Barnard & McManus (1973) have reported a decrease of the foraminifera–radiolaria ratio in Holocene sediment compared to Pleistocene deposits. In Middle Valley, the CaO content is lower in Holocene sediments and higher in Late Pleistocene sediments, and opaline silica displays the inverse trend (Blaise *et al.* 1988). Elements such as Ba, Cu and Zn, which are commonly associated with sediment of biogenic origin (Marchig *et al.* 1985, Bischoff *et al.* 1979) correlate with the high opaline silica layer in Middle Valley.

Important diagenetic reactions which have been studied in Recent sediments are illustrated schematically in Figure 15 (Kaplan *et al.* 1963, Goldhaber & Kaplan 1974, 1980, Goldhaber *et al.* 1977, Berner 1984, 1985, Trudinger *et al.* 1985). Element profiles of unmineralized cores from Middle Valley display characteristic trends: Mn, Fe^{3+}, Ba, Zn, Cu and Ni increasing upwards and reaching a maximum in brown surface layers, whereas Fe^{2+} and S^{2-} increase downwards (Fig. 7). The controlling reactions are biologically mediated and involve the reduction of sulfate to sulfide by bacteria which metabolize and oxidize organic carbon to carbonate in the process. Dissolved oxygen is usually consumed at depth within tens of cm of the seafloor and reducing conditions are established. Mn oxyhydroxides formed on the seafloor become reduced during burial; the dissolved Mn diffuses upward and precipitates in the thin oxidized zone. Elements such as Ni, Co, Pb and Cd, which are commonly bound by Mn oxyhydroxides (Balistrieri & Murray 1986), are likewise enriched in surface layers. Iron oxyhydroxides precipitated on the seafloor become reduced with burial; iron monosulfides are formed when this iron combines with sulfur derived from bacterial reduction of seawater sulfate. Downward decreases in the amount of dissolved sulfate may limit barite formation with depth in cores.

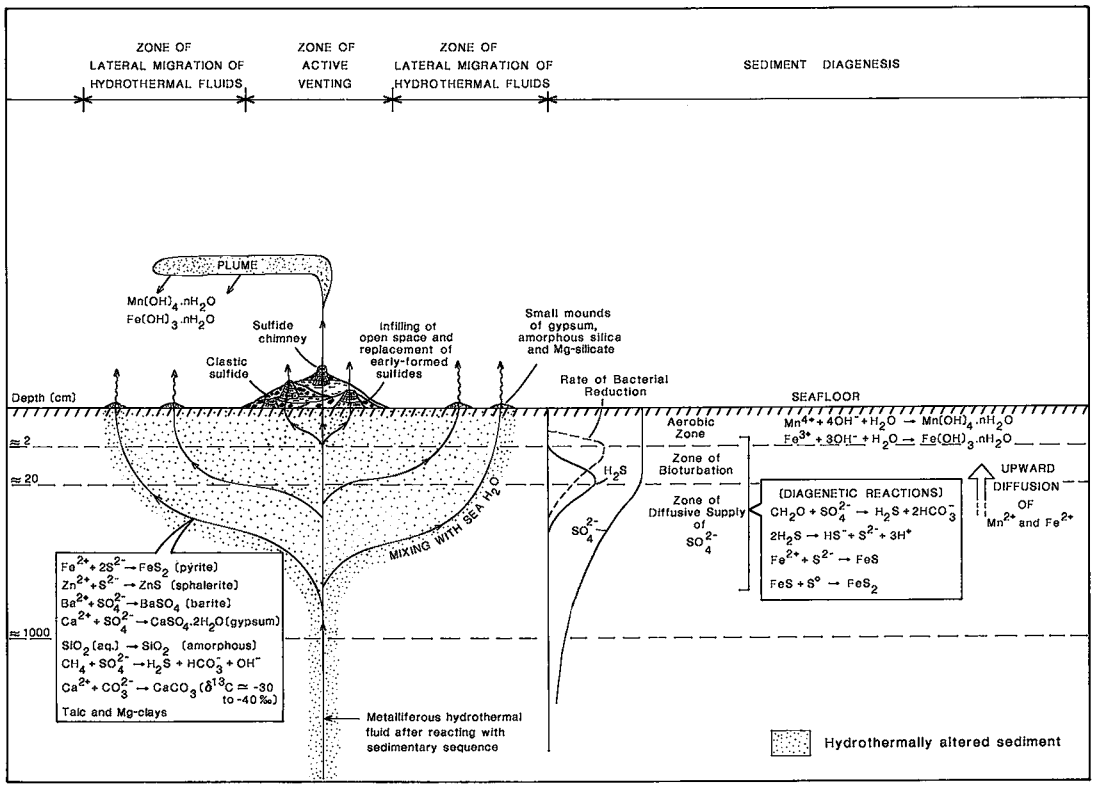

FIG. 15. Schematic model for the formation of hydrothermal mounds, Middle Valley. Basic chemical reactions in the hydrothermal alteration zone and relative changes in H_2S and SO_4^{2-} contents in pore waters are also shown. Evidence for lateral movement of hydrothermal fluids near the seafloor is provided by heat-flow transects across the Area of Active Venting.

Elements such as Mn, Fe, Zn and Ba, which are concentrated in sulfide deposits, may have originated in part from hydrothermal plumes, and have then been redistributed during diagenesis. Smoothing of element profiles during diagenesis would tend to destroy diagnostic evidence such as element spikes associated with hydrothermal pulses.

Hydrothermal alteration of sediment

Evidence for elevated temperatures has been provided by heat-flow surveys in the area (Davis & Villinger, in prep.). Using a sediment conductivity of 1W m^{-1} deg K^{-1}, the temperature gradient ranges from 2.5°C m^{-1} to 30°C m^{-1} over a lateral distance of about 100 m. The heat-flow profile is typically symmetrically distributed about the zone of maximum hydrothermal discharge. Areas of elevated heat flow situated adjacent to vents most likely represent zones where hydrothermal fluids migrated laterally from the conduit into the adjacent hemipelagic sediments.

Hydrothermally altered sediment cored from areas of high heat flow are typically more indurated and granular than unaltered sediment from Middle Valley, due to silica and carbonate cementation, and contain authigenic barite, gypsum, calcite (as nodules and cement), unidentified Mg-rich silicates and pyrite. In PAR 85-34, P, Cr, Fe, Cu and As are locally enriched compared to unaltered sediments from Middle Valley. The last three elements are most likely associated with pyrite, which is common throughout the cores; P is hosted by apatite.

For minerals with retrograde solubilities, such as gypsum, elevated temperatures generated by the advection of hydrothermal fluids through the sedimentary pile would be sufficient to cause precipitation from pore waters with a seawater composition. Gypsum dredged near the surface has a $^{87}Sr/^{86}Sr$ ratio of 0.70665, suggesting that a significant proportion of the Sr was derived from hydrothermal fluids which had leached a basaltic source. Because of the low content of volcanic detritus in Middle Valley sediments, this source was probably the underlying oceanic crust.

Highly negative $\delta^{13}C$ values (-30 to -40‰) in calcite from carbonate concretions suggest derivation of carbon from a methane source. Methanogenic carbonates with similar $\delta^{13}C$ values have been described by Hathaway & Degens (1969). Methane is a common product of the thermal maturation of organic matter in sediments (Gieskes *et al.* 1982), and is enriched in hydrothermal fluids which have reacted with sediments in the Guaymas Basin (Welhan & Craig 1982). Oxidation of methane to carbonate in Middle Valley sediments may have been caused by methanogenic bacteria. Reduction of sulfate to sulfide occurs during this process, which may explain the association of pyrite with carbonate concretions.

Magnesium-rich silicates, which occur at 180 cm depth in core PAR 85-34, have been found in numerous hydrothermal deposits, including massive sulfides from Middle Valley (Davis *et al.* 1987) and Guaymas Basin (Lonsdale *et al.* 1980). In the same core, Adshead (1987) determined the Mg silicate to be a saponite–talc mixed-layer clay; this clay may have formed by the hydration of talc (Sakamoto *et al.* 1982). Talc is generally considered to have formed by the mixing of SiO_2-rich hydrothermal fluid with Mg-rich seawater or pore waters.

Sulfide formation

The North Sulfide Mound represents the end product of a number of processes including 1) initial quenching or mixing of hydrothermal fluids with entrained seawater or pore water and the formation of sulfide chimneys at the seafloor and veins cutting the underlying sediments; 2) the replacement and infilling of early-formed sulfides by precipitates from a later and probably lower temperature hydrothermal fluid; and 3) the sedimentary reworking of sulfide chimneys and associated "feeder-pipe" mineralization.

Evidence of sulfide precipitation below the seafloor consists of veins of isocubanite that cut altered hemipelagic sediment in clasts from one distinctive unit in PAR 85-13, and the rimming of clasts by sulfides in other units.

At the seafloor, the quenching and mixing of hydrothermal fluids with seawater has resulted in the precipitation of an open network of hexagonal pyrrhotite tablets, wurtzite and Cu–Fe sulfides. This network of sulfide minerals then served as a substrate for partial infilling and replacement by sphalerite, pyrite, marcasite, barite, covellite and galena. Alternating bands of pyrite, sphalerite and various iron oxides including lepidocrocite, goethite, hematite and magnetite is evidence for episodic discharge of hydrothermal fluids from the same conduit, interrupted by periods of oxidation by seawater and perhaps lower temperature hydrothermal fluids.

Barite occurs either as subhedral grains interpenetrating with sulfide minerals in clasts from chimneys, or as rosettes hosted in hemipelagic sediment. In the former, it appears late in the paragenetic sequence, commonly as infillings of the interstices of the pyrrhotite network, and formed by mixing of barium of hydrothermal origin with sulfate derived from a mixture of seawater and oxidized sulfides. Values of $\delta^{34}S$ for barite, which range between 10‰ and 12‰, are consistent with a mixture of seawater sulfate and low $\delta^{34}S$ sulfur of hydrothermal origin; some oxidation of chimney sulfides may also have occurred. An intial $^{87}Sr/^{86}Sr$ ratio of 0.70540 in barite from the North Sulfide Mound likewise indi-

cates mixing of seawater and hydrothermal basaltic strontium. Authigenic barite in hemipelagic sediments was formed from hydrothermal fluids which migrated to the seafloor. The barite is commonly associated with Mg silicates such as talc. This association is also present in core PAR 85-34 collected in the Area of Active Venting.

Lonsdale *et al.* (1980) identified talc in a hydrothermal deposit in the Northern Trough of the Guaymas Basin, where it occurs as a crumbly, porous material which forms patches on the sediment surface. Peter (1986) examined hydrothermal vent deposits from the Southern Trough of the Guaymas Basin and noted a fibrous mineral intergrown with fine-grained sulfides, mostly pyrrhotite. Talc and chrysotile form a distinct layer at the contact between chalcopyrite and anhydrite in chimneys from the EPR, 21°N (Goldfarb *et al.* 1983).

In the North Sulfide Mound, most of the talc and Mg-rich silicates have formed authigenically or as a replacement of hemipelagic sediment. Talc, which is generally considered to form by the mixing of SiO_2-rich and Mg-depleted hydrothermal fluid with seawater, has been predicted using incremental reaction models for mixing between hydrothermal fluids and seawater (Janecky & Seyfried 1984, Bowers *et al.* 1985). Talc was shown to be supersaturated over a large temperature range because sluggish kinetics retarded its precipitation. Slow reaction kinetics may explain the low talc content of most sulfide chimneys.

High contents of talc in Middle Valley probably resulted from the conductive cooling of hydrothermal fluids in the sediment column and sulfide mounds. This would reduce the kinetic problems and is consistent with its association with amorphous silica which has been shown by Janecky & Seyfried (1984) to form only by conductive cooling of a hydrothermal fluid.

Sulfides forming chimneys and "feeder" veins have been redeposited with hydrothermally altered hemipelagic sediment, Mg-rich silicates, and barite in gravity flows south of the North Sulfide Mound. The dominant factors controlling the formation of flows were unstable slopes and chimney structures due to oxidation, a substrate for sulfide chimneys which consisted of soft and structurally unstable hemipelagic sediment, and perhaps episodic seismic activity which would serve to trigger the collapse of chimneys and the shedding of gravity flows. Stacked sulfide debris flows which have been photographed in the area of one mound, and the occurrence of sulfide chimney textures in clastic units from core PAR 85-13, support this interpretation (Davis *et al.* 1987).

Hydrothermal fluid evolution

Although the evolution of Middle Valley hydrothermal fluids is probably complex and fluid compositions cannot be constrained precisely, it is possible to make some deductions based on the mineralogy and isotope chemistry. Initial $^{87}Sr/^{86}Sr$ ratios in barite and gypsum indicate that Middle Valley hydrothermal fluids are highly evolved and represent components of basaltic crust and sediments or seawater (or both). This is consistent with the lead isotope results which indicate a mixture of basaltic and sedimentary sources (Goodfellow *et al.* 1987). Highly positive $\delta^{34}S$ values in sulfides suggest that the sulfur likewise represents a mixture of primitive sulfur leached from the basaltic crust, and seawater sulfate abiotically reduced to sulfide at temperatures >250°C which have been estimated from heat-flow measurements (Davis *et al.* 1987) for the basal portions of the sedimentary pile. The source of sulfate may be seawater trapped in turbidite units, or seawater recharged into permeable units under a geothermal gradient.

Based on the isotopic results, it seems likely that the fluids from which the Middle Valley sulfides precipitated represented an end-member-type basalt-equilibrated hydrothermal fluid (Von Damm *et al.* 1985a) which exited the oceanic crust and reacted with the sedimentary pile. The magnitude of ^{34}S enrichment in sulfides over basaltic sulfur suggests that these fluids have been extensively modified by sediment reactions. Expected changes in the fluid chemistry include an increase in pH due to buffering by the clay–feldspar assemblage present in hemipelagic sediment; a pH increase would promote the precipitation of sulfides in the sedimentary pile. Reaction of an end-member fluid with sediments has been invoked by Von Damm *et al.* (1985b) to account for a marked increase in pH for hydrothermal fluids in the Guaymas Basin. The mixing with dissolved sulfide formed by abiotic reduction of sulfate in the sedimentary pile would also promote sulfide precipitation by increasing the fS_2. Methane generated by the thermal degradation of organic matter would lower the fO_2 of the fluid and may account for the initial predominance of pyrrhotite over pyrite in chimney sulfides from Middle Valley. The replacement of pyrrhotite by pyrite in chimney sulfides indicates that the fO_2 increased after the initial precipitation of pyrrhotite, perhaps due to the entrainment of seawater.

Conclusions

1. Eight mound-like structures are visible on seabeam bathymetric and SeaMARC II maps of Middle Valley. These mounds form linear arrays oriented NNE–SSW and range up to 2 km in diameter and 100 m high. Both seismic and 3.5 kHz acoustical profiles of mounds show them to be transparent except for discontinuous reflectors and a thin veneer of sediment at the surface (Davis *et al.* 1987). Two

areas in Middle Valley display anomalously high heat flow, the southern margin of the North Sulfide Mound, and the Area of Active Venting located 3 km to the northwest. Massive sulfides have been cored and dredged from one mound (North Sulfide Mound). Piston, gravity, and boomerang coring of three additional mounds have recovered only unaltered hemipelagic sediment. If sulfides occur in these mounds, they are probably concealed below a cover of hemipelagic sediment.

2. The absence of strong acoustical reflectors on 3.5 kHz profiles in the Area of Active Venting where mounds are absent suggests that the sediment layering was obliterated by hydrothermal processes. Sediments from the area are in fact indurated with silica and calcite cements, and with other hydrothermal minerals including barite, Mg-rich silicates, gypsum, pyrite and calcite.

3. The mounds in Middle Valley formed by construction of a substrate which was later infilled and replaced to variable degrees by hydrothermal products. This substrate consisted initially of crumbled sulfide chimneys, other hydrothermal products such as barite and Mg silicates, and hemipelagic sediment. With the buildup of mounds and the establishment of unstable slopes, gravity flows composed of chimney sulfides, "feeder" mineralization, and hemipelagic sediment were shed off the margins. Fluids trapped in the open space within this permeable and highly porous substrate would have time to conductively cool and precipitate minerals that have sluggish kinetics, such as amorphous silica and talc.

4. Clasts of chimney sulfides consist of an open network of hexagonal pyrrhotite, wurtzite (now inverted to sphalerite) and isocubanite (with chalcopyrite lamellae) which has been infilled and variably replaced by pyrite, marcasite, covellite, galena, amorphous silica and barite. "Feeder" mineralization consists of Cu–Fe sulfide veins that cut hydrothermally altered hemipelagic sediment.

5. Sulfides from Middle Valley probably formed from hydrothermal fluids which evolved by reacting with the sedimentary pile. This is indicated by 1) highly positive $\delta^{34}S$ values for sulfides; 2) initial $^{87}Sr/^{86}Sr$ ratios for barite and gypsum that plot between values for MORBs and continentally derived sediments or seawater; and 3) high pyrrhotite/pyrite ratios which are consistent with a low fO_2 generated by reaction with sedimentary organic matter.

6. Reaction of an end-member-type hydrothermal fluid exiting the oceanic crust with the feldspar–clay assemblage in Middle Valley sediments would be expected to increase the pH and result in the precipitation of sulfides. Middle Valley, therefore, has the potential to host sulfides in the sedimentary pile as well as in mounds.

7. Middle Valley sediments serve as an impervious, insulating cap which reduces conductive and convective heat loss, thereby sustaining a prolonged hydrothermal system. This thermal regime therefore is conducive to the formation of large sulfide deposits at a restricted number of long-lived vent sites.

Acknowledgements

The authors are grateful to Chief Scientists E.E. Davis and B.D. Bornhold for planning and organizing the cruise and for stimulating scientific discussions of Middle Valley, to R. Macdonald and K. Conway for their assistance with sediment coring, and Captain P. Frost and the officers and crew of *C.H.S. PARIZEAU* for their cooperation and expert seamanship. In addition, we thank G.M. LeCheminant and D. Walker for mineralogical assistance, G.R. Lachance and G.E.M. Hall for organizing chemical analyses, and B. Taylor for overseeing sulfur isotope analyses. J. Shaw, A. Douma, B. Price and B. Sawyer assisted with the computer plotting and drafting of diagrams. Helpful reviews were provided by I.R. Jonasson, J.M. Franklin, T. Barrett, B.D. Bornhold, and an anonymous reviewer. This is G.S.C. Contribution 39487.

References

Adshead, J.D. (1987): Magnesium distribution and the nature of magnesian silicates in hydrothermally-altered Juan de Fuca sediments. *Amer. Geophys. Union Trans. Program Abstr.* **68,** 113.

Al-Aasm, I.S. & Blaise, B. (1987): Hydrothermal fluid efects on the sediment column in Middle Valley, Juan de Fuca Ridge (N.E. Pacific). *Amer. Assoc. Petrol. Geol. Program Abstr.* 20.

Arnold, M. & Sheppard, S.M.F. (1981): East Pacific Rise at latitude 21°N: isotopic composition and origin of hydrothermal sulfur. *Earth Planet. Sci. Lett.* **56,** 148-156.

Baker, E.T., Feeley, R.A. & Massoth, G.J. (1987): Hydrographic and chemical survey of hydrothermal plumes from the Middle Valley vent field, Juan de Fuca Ridge, *EOS, Trans. Amer. Geophys. Union* **84,** 1325.

Balistrieri, L.S. & Murray, J.W. (1986): The surface chemistry of sediments from the Panama Basin: The influence of Mn oxides on metal absorption. *Geochim. Cosmochim. Acta* **50,** 2235-2243.

Barnard, W.D. & McManus, D.A. (1973): Planktonic foraminiferan–radiolarian stratigraphy and the Pleistocene–Holocene boundary in the Northeast Pacific. *Geol. Soc. Amer. Bull.* **84,** 2097-2100.

BARRON, E.J. & WHITMAN, J.M. (1981): Oceanic sediments in space and time. *In* The Sea (C. Emiliani, ed.). John Wiley & Sons, New York.

BERNER, R.A. (1984): Sedimentary pyrite formation: An update. *Geochim. Cosmochim. Acta* **48**, 605-615.

_____ (1985): Sulfate reduction, organic matter decomposition and pyrite formation. *Phil. Trans. Roy. Soc. London* **A315**, 25-38.

BISCHOFF, J.L., HEATH, G.R. & LEINEN, M. (1979): Geochemistry of deep sea sediments from the Pacific manganese nodule province-domes sites A, B, and C. *In* Marine Geology and Oceanography of the Pacific Manganese Nodule Province (J.L. Bischoff & D.Z. Piper, eds.). Plenum, New York.

BLAISE, B. (1985): *Sédimentation et Paléoenvironnements Plio-Quaternaires sur la Bordure Nord-Est de l'Océan Pacifique.* Université Sciences Techniques Lille, France, Thèse 3^{emc} cycle.

_____, BORNHOLD, B.D., MAILLOT, H. & CURRIE, R.G. (1984): Sedimentation near the Dellwood Knolls, Northern Juan de Fuca Ridge system. *EOS, Trans. Amer. Geophys. Union* **65**, 1112.

_____, _____, _____ & CHAMLEY, H. (1985): Observations sur les environnements Recents au nord de la Dorsale de Juan de Fuca (Pacifique nord-est). *Rev. Geol. Dyn. Geogr. Phys.* **26**, 201-213.

_____ & _____ (1987): Geochemistry of Northern Juan de Fuca Ridge sediments, northeast Pacific. *Geol. Surv. Can. Pap.* **87-1A**, 127-142.

_____, _____, CONWAY, K.W. & KARLIN, R.H. (1988): Glacial history and deep sea sedimentation in the Northeast Pacific since 38,000 BP. *Geol. Assoc. Can. - Mineral. Assoc. Can. Program Abstr.* **13**, 11.

BOWERS, T.S., VON DAMM, K.L. & EDMOND, J.M. (1985): Chemical evolution of mid-ocean ridge hot springs. *Geochim. Cosmochim. Acta* **49**, 2239-2252.

BURKE, W.H., DENISON, R.E., HETHERINGTON, E.A., KOEPNICK, R.B., NELSON, H.F. & OTTO, J.B. (1982): Variation of seawater $^{87}Sr/^{86}Sr$ throughout Phanerozoic time. *Geology* **10**, 516-519.

CHAMLEY, H. (1971): *Recherches sur la Sédimentation Argileuse en Méditerranée.* Thèse Science, Université Aix-Marseille, France.

CURRAY, J.R. & MOORE, D.G. (1982): *Initial Reports of Deep Sea Drilling Project* **64**,1119. U.S. Gov. Printing Office, Washington, D.C.

DAVIS, E.E. & LISTER, C.R.B. (1977): Tectonic structures on the Juan de Fuca Ridge. *Geol. Soc. Amer. Bull.* **88**, 346-363.

_____, CURRIE, R., SAWYER, B., RIDDIHOUGH, R. & HOLMES, M. (1985): Juan de Fuca Ridge atlas: Seamarc II acoustic image mosaic (Northern Juan de Fuca Ridge). *Geol. Surv. Can. Open File* **1144.**

_____ & SAWYER, B. (1987): Marine geophysical maps of western Canada. *Geol. Surv. Can.*, bathymetric map **6-1987.**

_____, GOODFELLOW, W.D., BORNHOLD, B.D., ADSHEAD, J., BLAISE, B., VILLINGER, H. & LE CHEMINANT, G. (1987): Massive sulphides in a sedimented rift valley, Northern Juan de Fuca Ridge. *Earth Planet. Sci. Lett.* **82**, 49-61.

GIESKES, J.M., ELDERFIELD, H., JOHNSON, J., MEYERS, B. & CAMPBELL, A. (1982): Geochemistry of interstitial waters and sediments, Leg 64, Gulf of California. *Initial Reports of Deep Sea Drilling Project* **64**, 675-694. U.S. Gov. Printing Office. Washington, D.C.

GOLDFARB, M.S., CONVERSE, D.R., HOLLAND, H.D. & EDMOND, J.M. (1983): The genesis of hot spring deposits on the East Pacific Rise, 21°N. *Econ. Geol. Monogr.* **5**, 184-197.

GOLDHABER, M.B., ALLER, R.C., COCHRAN, J.K., ROSENFELD, J.K., MARTENS, G.S. & BERNER, R.A. (1977): Sulfate reduction, diffusion and bioturbation in Long Island Sound sediments: Report of the FOAM Group. *Amer. J. Sci.* **277**, 193-237.

_____ & KAPLAN, I.R. (1974): The sulfur cycle. *In* The Sea **5** (E.D. Goldberg, ed.). Wiley-Interscience, New York, 569-655.

_____ & _____ (1980): Mechanisms of sulfur incorporation and isotope fractionation during early diagenesis in sediments of the Gulf of California. *Mar. Chem.* **9**, 95-143.

GOODFELLOW, W.D., JONASSON, I.R., BLAISE, B., FRANKLIN, J.M. & GRAPES, K. (1987): Nature of sulfide-rich mounds in sediment-filled Middle Valley, Northern Juan de Fuca Ridge. *EOS, Trans. Amer. Geophys. Union Trans. Program Abstr.* **68**, 1546.

HATHAWAY, J.C. & DEGENS, E.T. (1969): Methane-derived marine carbonates of Pleistocene age. *Science* **165**, 690-692.

HOLTZAPFFEL, T. (1985): Les minéraux argileux: préparation, analyse diffractométrique et détermination. *Ann. Soc. Geol. Nord Mem.* **12.**

JANECKY, D.R. & SEYFRIED, W.E., JR. (1984): Formation of massive sulfide deposits on oceanic ridge crests: Incremental reaction models for mixing between hydrothermal solutions and seawater. *Geochim. Cosmochim. Acta* **48**, 2723-2738.

KAJIWARA, Y. & KROUSE, H.R. (1971): Sulphur isotope

partitioning in metallic sulphide systems. *Can. J. Earth Sci.* **8,** 1397-1408.

KAPLAN, I.R., EMERY, K.O. & RITENBERG, S.D. (1963): The distribution and isotopic abundances of sulphur in Recent marine sediments off southern California. *Geochim. Cosmochim. Acta* **27,** 297-331.

KARSTEN, J.L., HAMMOND, S.R., DAVIS, E.E. & CURRIE, R. (1986): Detailed geomorphology and neotectonics of the Endeavor segment, Northern Juan de Fuca Ridge. New results from Seabeam swath mapping. *Geol. Soc. Amer. Bull.* **97,** 213-221.

KASTNER, M. (1982): Evidence for two distinct hydrothermal systems in the Guaymas Basin. *Initial Reports of Deep Sea Drilling Project* **64,** 1143-1157. U.S. Gov. Printing Office, Washington, D.C.

KERRIDGE, J., HAYMON, R.M. & KASTNER, M. (1983): Sulfur isotope systematics at the 21°N site, East Pacific Rise. *Earth Planet. Sci. Lett.* **66,** 91-100.

KIYOSU, Y. (1980): Chemical reduction and sulfur-isotope effects of sulfate by organic matter under hydrothermal conditions. *Chem. Geol.* **30,** 47-56.

LONSDALE, P., BISCHOFF, J.L., BURNS, V.M., KASTNER, M. & SWEENEY, R.E. (1980): A high-temperature hydrothermal deposit on the seabed at a Gulf of California spreading center. *Earth Planet. Sci. Lett.* **49,** 8-20.

MARCHIG, V., MOLLER, P., BACKER, H. & DULSKI, P. (1985): Foraminiferal ooze from the Galapagos Rift area – hydrothermal impact and diagenetic mobilization of elements. *Mar. Geol.* **62,** 85-104.

MCCOY, F.W. & SANCETTA, C. (1985): North Pacific sediments. *In* The Ocean Basins and Margins **7A** (A.E.M. Nairn, F.G. Stehli & S. Uyeda, eds.). Plenum Press, New York, 1-64.

O'NIONS, R.K. & PANKHURST, R.J. (1973): Secular variations in the Sr-isotope composition of Icelandic volcanic rocks. *Earth Planet. Sci. Lett.* **21,** 13-21.

PETER, J.M. (1986): *Genesis of Hydrothermal Vent Deposits in the Southern Trough of Guaymas Basin, Gulf of California: a Mineralogical and Geochemical Study.* M.Sc. thesis, Univ. Toronto, Toronto, Ontario.

REES, C.E. (1978): Sulfur isotope measurements using SO_2 and SF_6. *Geochim. Cosmochim. Acta* **42,** 383-389.

SAKAI, H., DES MARAIS, D.J., UEDA, A. & MOORE, J.G. (1984): Concentrations and isotope ratios of carbon, nitrogen and sulfur in ocean-floor basalts. *Geochim. Cosmochim. Acta* **48,** 2433-2441.

SAKAMOTO, T., KOSHIMIZU, H., SHINODA, S. & OTSUKA, R. (1982): Hydrothermal transformation of some minerals into stevensite. *In* Developments in Sedimentology (H. Van Olphen & F. Veniale, eds.), **35,** 537-543.

SASAKI, A., ARIKAWA, Y. & FOLINSBEE, R.E. (1979): Kiba reagent method of sulphur extraction applied to isotopic work. *Bull. Geol. Surv. Japan* **30,** 241-245.

SHANKS, W.C., III & SEYFRIED, W.E., JR. (1987): Stable isotope studies of vent fluids and chimney minerals, southern Juan de Fuca Ridge: Sodium metasomatism and seawater sulfate reduction. *J. Geophys. Res.* **92,** 11387-11399.

STYRT, M.M., BRACKMANN, A.J., HOLLAND, H.D., CLARK, B.C., PISUTHA-ARNOND, V., ELDRIDGE, C.S. & OHMOTO, H. (1981): The mineralogy and composition of sulphur in hydrothermal sulphide/sulphate deposits on the East Pacific Rise, 21°N Latitude. *Earth Planet. Sci. Lett.* **53,** 382-390.

SUBBARAO, K.V. & HEDGE, C.E. (1973): K, Rb, Sr and $^{87}Sr/^{86}Sr$ in rocks from the Mid-Indian oceanic ridge. *Earth Planet. Sci. Lett.* **18,** 223-226.

TRUDINGER, P.A., CHAMBERS, L.A. & SMITH, J.W. (1985): Low-temperature sulphate reduction: biological versus abiological factors. *Can. J. Earth Sci.* **22,** 1910-1918.

VILLINGER, H. & DAVIS, E.E. (1986): Hydrothermal regime of a sedimented rift valley, northern Juan de Fuca Ridge. *EOS, Trans. Amer. Geophys. Union* **67,** 1232.

VON DAMM, K.L., EDMOND, J.M., GRANT, B., MEASURES, C.I., WALDEN, B. & WEISS, R.F. (1985a): Chemistry of submarine hydrothermal solutions at 21°N, East Pacific Rise. *Geochim. Cosmochim. Acta* **49,** 2197-2220.

_____, MEASURES, C.I. & GRANT, B. (1985b): Chemistry of submarine hydrothermal solution at Guaymas Basin, Gulf of California. *Geochim. Cosmochim. Acta* **49,** 2221-2238.

WELHAN, J.A. & CRAIG, H. (1982): Abiogenic methane in mid-ocean ridge hydrothermal fluids. *In* Deep Source Gas Workshop Tech. Proc. (W.J. Guillian, ed.). Morgantown, W. Virginia, 122-129.

ZIERENBERG, R.A., KOSKI, R.A., SHANKS, W.C., III & ROSENBAUER, R.J. (1986): Form and composition of sediment-hosted sulfide deposits, Escanaba Trough, Southern Gorda Ridge. *EOS, Trans. Amer. Geophys. Union* **67,** 1282.

Received August 18, 1987; revised manuscript accepted May 14, 1988.